



## More than agriculture: Analysing time-cumulative human impact on European land-cover of second half of the holocene

Anhelina Zapolska<sup>a,\*</sup>, Maria Antonia Serge<sup>b</sup>, Florence Mazier<sup>b</sup>, Aurélien Quiquet<sup>c</sup>, Hans Renssen<sup>d</sup>, Mathieu Vrac<sup>c</sup>, Ralph Fyfe<sup>e</sup>, Didier M. Roche<sup>a,c</sup>

<sup>a</sup> Earth and Climate Cluster, Faculty of Science, Vrije Universiteit Amsterdam, 1081, HV, Amsterdam, the Netherlands

<sup>b</sup> Laboratoire Géographie de L'Environnement, UMR 5602, CNRS, Université de Toulouse-Jean Jaurès, 31058, Toulouse, France

<sup>c</sup> Laboratoire des Sciences Du Climat et de L'Environnement, LSCE/IPSL, CEA-CNRS-UVSQ, Université Paris-Saclay, 91190, Gif-sur-Yvette, France

<sup>d</sup> Department of Natural Sciences and Environmental Health, University of South-Eastern Norway, 3800, Bø, Norway

<sup>e</sup> School of Geography, Earth and Environmental Sciences, University of Plymouth, PL4 8AA, Plymouth, UK

### ARTICLE INFO

Handling Editor: Donatella Magri

#### Keywords:

Anthropogenic land-cover change  
Climate-forced vegetation modelling  
Pollen-based reconstructions  
Europe

### ABSTRACT

Assessment of past anthropogenic modifications of land-cover dynamics is key to understanding the human role in the Earth system. Recent advances in palaeoenvironmental sciences allow us to assess the long-term impacts of anthropization on ecosystems, landscapes, and land-cover.

Our study aims to evaluate the role of human impact on European land-cover over the past 6000 years by comparing two independent datasets. First, we use a dynamic vegetation model forced by debiased climate model outputs. The climate model uses natural forcings only and therefore the computed vegetation distribution is interpreted as the potential natural vegetation. Second, we use pollen-based reconstructions, which intrinsically include anthropogenic influence. The discrepancies between the two datasets are attributed to human activity and quantified in a form of a human pressure index (HPI).

Patterns of spatio-temporal evolution of the HPI agree with previously published data about the spread of agriculture in Europe. In particular, both HPI and anthropogenic land-cover change (ALCC) scenarios indicate a rapid increase of the human pressure around 1200–1700 BP, and a significant increase of agriculture-related land-cover modifications by nearly 60% throughout the second half of the Holocene. However, initially high HPI values (up to 70%) at 5700–6200 BP, which correlate with population estimates ( $r = 0.75$ ,  $p$ -value  $< 0.005$ ), suggest high levels of anthropogenic land-cover transformations, introduced by earlier agricultural as well as non-agricultural activities.

The results of our study suggest that vegetation cover of the Mid-Holocene substantially differed from the state of potential natural vegetation (PNV) due to cumulative effect of early human alterations on the land-cover. This challenges the hypothesis that vegetation in the Mid-Holocene was in a relatively natural state and contributes valuable insights to the onset of agriculture as the start of the Anthropocene.

### 1. Introduction

Numerous scholars, particularly within the geological community, mark the start of the Anthropocene by the transition to fossil fuel burning, artificial radionuclides spread by the thermonuclear bomb tests or rapid changes in the biosphere, which typically begin between the Industrial Revolution (ca. 1800 CE) and the early 1950s (Bauer et al., 2021; Crutzen, 2002; Head et al., 2022a; Steffen et al., 2011; Waters et al., 2016; Zalasiewicz et al., 2021). However, in recent years

researchers propose to account for the emergence of humanity as a force on Earth's landscape. Scholars in archaeological and palaeoecological communities argue that humans begun substantially impacting the environment several thousands of years earlier than previously suggested (Braje and Erlandson, 2013b; Ellis et al., 2021; Erlandson and Braje, 2013; Lightfoot and Cuthrell, 2015; Nikulina et al., 2022; Smith and Zeder, 2013). It is thus debatable whether Anthropocene's "golden spike" should be marked by the appearance of anthropogenic soils (Certini and Scalenghe, 2011), onset of agriculture (Ruddiman, 2013),

\* Corresponding author.

E-mail address: [a.zapolska@vu.nl](mailto:a.zapolska@vu.nl) (A. Zapolska).

<https://doi.org/10.1016/j.quascirev.2023.108227>

Received 15 May 2023; Received in revised form 28 June 2023; Accepted 12 July 2023

0277-3791/© 2023 The Authors. Published by Elsevier Ltd. This is an open access article under the CC BY license (<http://creativecommons.org/licenses/by/4.0/>).

late Pleistocene megafaunal extinctions (Braje and Erlandson, 2013a), or defining the “Anthropocene” term should be omitted altogether and used as a flexible term instead (Edgeworth et al., 2015; Ruddiman, 2018; Rull, 2017; Swindles et al., 2023). Moreover, other terminology was proposed to define early hominin impact on the environment, such as the Palaeoanthropocene (Foley et al., 2013). To address the challenges associated with formalizing the Anthropocene as a distinct epoch (sub-division of the Geological Time Scale), recent studies suggest to define the Anthropocene as an ongoing event (Edwards et al., 2022; Gibbard et al., 2022; Bauer et al., 2021) or episode (Head et al., 2022b), rather than an epoch. In any case, in the light of the Anthropocene discussion, the history of anthropogenic impact on land-cover became a key topic in palaeoenvironmental studies.

The role of land-cover modifications attributed to human activity over the Holocene is often quantified by means of anthropogenic land-cover change (ALCC) models (HYDE 3.2: Goldewijk et al., 2017a; KK10: Kaplan et al., 2009; Pongratz et al., 2008). While their reliability is largely limited by a number of factors, such as not explicitly accounting for effects of Holocene climate or geomorphic change and variability, and uncertainties in the underlying data, ALCC models are currently the only available method to produce spatially- and temporally-continuous data of numerically expressed human-environment interactions (Kaplan et al., 2017). These models are based on historical human population density estimates, the land needed to sustain that population, and its suitability, determined by climate and soil properties (Kaplan et al., 2009; Pirzamanbein and Lindström, 2022). However, ALCC models, such as KK10 or HYDE 3.2, do not yet incorporate archaeological and palaeoecological proxy data or historical descriptions of past land use (Trondman et al., 2015). Several approaches have been developed to estimate past ALCCs to assess their possible effects on past land-cover (Ramankutty and Foley, 1999; Olofsson and Hickler, 2008; Pongratz et al., 2008, 2010; Kaplan et al., 2009, 2011; Lemmen, 2009; Goldewijk et al., 2011). While existing ALCC scenarios (Goldewijk et al., 2017a; Kaplan et al., 2009; Pongratz et al., 2008) significantly differ from each other (Gaillard et al., 2010; Kaplan et al., 2017), they all tend to represent anthropogenic impact centred around agricultural activities. For example, multiple studies focus on their representation of the onset and adoption of agriculture in different ALCC scenarios (Smith et al., 2016; Stephens et al., 2019; Stocker et al., 2011; Vavrus et al., 2022). KK10 in particular, features deforestation for crop cultivation and pastures to quantify human influence on land-cover (Kaplan et al., 2009). However, deforestation by humans is not limited to agricultural purposes. Harrison et al. (2020), and even Kaplan et al. (2017) themselves highlighted the need for inclusion of non-agricultural activities in the analysis of spatial patterns of anthropogenic land use.

Furthermore, while human impact on the environment intensified with the introduction of agriculture, pre-agricultural landscapes were already far from “natural” or “intact” (Ellis et al., 2021). Humans have a long history of shaping their environments through niche construction activities (Nikulina et al., 2022), for example through burning (Scherjon et al., 2015), and geographic range manipulations of plant and animal species (Finsinger et al., 2006; Rowley-Conwy and Layton, 2011). Such alterations had a smaller immediate effect on the environment compared to agriculture, especially industrial practices, but niche-constructing activities spanned many thousands of years, dating back as far as the Last Interglacial (Roebroeks et al., 2021), with numerous studies reporting cases of land-cover modifications over late Pleistocene and early Holocene (Archibald et al., 2012; Bos and Urz, 2003; Doughty, 2013; McWethy et al., 2010; Pinter et al., 2011; Roberts et al., 2021). Therefore, the cumulative effect of the prehistory-long legacy of non-agricultural human practices on land-cover remains poorly understood.

Quantitative reconstructions of past vegetation cover indicate that changes of vegetation in Europe reach maximum complexity in terms of the rate of change during the second half of the Holocene (from 8200 to

4200 BP to present day; hereafter, dates are expressed as calibrated calendar years before 1950 CE and referred to as BP) (Marquer et al., 2014; Mottl et al., 2021). In Europe this period is characterized by the adoption of agriculture and intensification of human-induced land-cover change (Stephens et al., 2019; Morrison et al., 2021; Harrison et al., 2020; Goldewijk et al., 2017a; Kaplan et al., 2011; Gronenborn and Horejs, 2021) as well as by a substantially changing climate (Arthur et al., 2022; Zhang et al., 2017). Moreover, analysis of the European Pollen Database indicated that anthropogenic land-cover change in pollen records becomes detectable from 6000 BP (Fyfe et al., 2015). Hence, in this study we focus on quantifying the anthropogenic impact on European land-cover over the period of the second half of the Holocene (6200 CE).

Estimation of the magnitude of human-induced changes in land-cover is often performed through analysis of palaeoecological data acquired from pollen-based reconstructions (Bartlein et al., 2011; Dallmeyer et al., 2019; Marquer et al., 2017; Prentice et al., 1998; Strandberg et al., 2022). One of such reconstructions, the Regional Estimates of VEgetation Abundance from Large Sites (REVEALS) model (Sugita, 2007a), was used to create gridded pollen-based estimates of Holocene plant cover for NW-central Europe north of the Alps (five time windows of the Holocene) (Trondman et al., 2015) and more recently for all of Europe through the Holocene (11,700 BP to present) (Githumbi et al., 2022). The REVEALS reconstructions from Marquer et al. (2017) have been used in the recent study of Dallmeyer et al. (2023), who applied an approach based on the comparison between REVEALS-based reconstructions and land use forced vegetation model outputs for northern and central Europe. Their study concluded that anthropogenic land use was the main driver of the decrease in forest cover in Europe during mid- and late-Holocene (100–8000 BP). To further this analysis, we simulate vegetation for the second half of the Holocene (6200 CE) and compare the results with an extended version of the REVEALS-based reconstructions (Serge et al., 2023). Serge et al. (2023) used the same protocol as described in Githumbi et al. (2022) to produce the most spatially extensive and temporally continuous pollen-based reconstructions of plant cover in Europe (at a spatial resolution of  $1^\circ \times 1^\circ$  for  $30^\circ\text{--}71^\circ\text{ N}$ ,  $20^\circ\text{ W--}47^\circ\text{ E}$ ; spatial distribution is shown in Fig. 2) over the Holocene at a temporal resolution of 500 years between 11,700 and 700 BP. For the most recent period, Serge et al. (2023) allocated smaller time windows with a higher temporal resolution: 700–350 BP, 350–100 BP, and 100 BP–present (where the present is the year of coring).

While indicating the significance of land use as a key factor in driving past land-cover change in Europe, Dallmeyer et al. (2023) highlighted several challenges that arise when comparing pollen-based quantitative vegetation reconstructions with outputs from vegetation models. In our current study, we address two of these challenges: biases in simulated climate and distinction between anthropogenic and non-anthropogenic drivers of land-cover change. To overcome these challenges, we propose a method that compares pollen-based reconstructions with a theoretical state of vegetation cover - potential natural vegetation (PNV), which represents climate-forced vegetation without human intervention or management (Hengl et al., 2018).

In this study, by analysing relationships between simulated PNV and pollen-based estimates of regional vegetation abundance, we aim to (1) evaluate how far from natural conditions our REVEALS-based vegetation is, by comparison with modelled potential natural vegetation, (2) quantify time-cumulative impact of human modifications of European land-cover (accumulated impacts of human activity on natural ecosystems through time) over the second half of the Holocene (6200 CE) including both agricultural and non-agricultural human activities, and (3) assess the performance of the developed methodology through comparison with existing ALCC scenarios KK10 and HYDE 3.2.

## 2. Methodology

### 2.1. Study design

In this study, we address the challenge of distinguishing between anthropogenic and non-anthropogenic drivers of land-cover change. Pollen-based land-cover reconstructions allow the identification of phases of vegetation compositional change comparable with periods of climate change, derived from independent climate reconstructions to account for the importance of climate-driven vegetation change (Seddon et al., 2014). However, the interaction of natural forces with anthropogenic influences induces complex processes with profound effects on the environmental system (Kalis et al., 2003). It is thus not always easy to attribute temporal changes in vegetation composition to a certain impact factor. The complex nature of interactions between different impact factors often makes it difficult to distinguish between climatic and anthropogenic origin of changes in vegetation patterns. Anthropogenic impact on vegetation composition is often derived from pollen-based reconstructions using cultural indicators (e.g. Deza-Araujo et al., 2020; Behre, 1981). The applicability of these indicators has been limited to regional studies due to regional variations in cultural practices and vegetation dynamics. Recently, Deza-Araujo et al. (2022) suggested the use of agricultural land use probability (LUP) index based on existing cultural indicators. This approach allows the use of the method beyond the specific regions where the cultural indicators were developed. However, while promising, its application to continental scales has not been explored. The relative importance of different impact factors for various regions and time periods is, therefore, still a matter of debate (Marquer et al., 2017; Dallmeyer et al., 2023). Moreover, quantifying the effect of early non-agricultural human practices (such as burning, wood harvesting for different purposes, settlement activities, and geographic range manipulations of species) on land-cover remains a challenging task, since these practices cannot be retrieved using cultural indicators that target agricultural land use through the presence of representative taxa in pollen records, i.e. Cerealia type (t.) (e.g. Githumbi et al., 2022; Gaillard, 2007). To tackle these challenges, analysis of pollen-based reconstructions would benefit from comparison to a reference state that would represent vegetation over the studied time period without anthropogenic changes of vegetation. Thus, in order to evaluate the extent of human-induced land-cover change in Europe during the second half of the Holocene (6200 CE), we applied a method that compares vegetation cover obtained through REVEALS-based reconstructions with an alternative description of past vegetation cover – potential natural vegetation (PNV). The concept of PNV has been the subject of past debate (e.g. Loidi et al., 2010; Jackson, 2013; Hengl et al., 2018; Somodi et al., 2012; Farris et al., 2010). We consider that PNV describes a theoretical state of vegetation cover that would exist under the assumption that the vegetation is in balance with environmental controls, such as climatic conditions and disturbances, without any human intervention or management (Hengl et al., 2018). In a palaeoenvironmental modelling context, PNV is often referred to an artificial construct simulated by a dynamic vegetation model (DVM) without prescribed land use forcing, that represents climate-forced potential vegetation in the absence of human-induced vegetation changes and other disturbances (e.g. wildfire, megafauna) (Trondman et al., 2015). PNVs are routinely used in various modelling exercises, such as to evaluate vegetation naturalness (Strona et al., 2016), analyse response of vegetation to climate change (Ren et al., 2021), or evaluate reconstructions of past regional vegetation patterns (Cruz-Silva et al., 2022). A PNV distribution is often simulated by vegetation models, which are based on modern empirical relationships between vegetation and climate (Levvasseur et al., 2013). Taking advantage of the PNV concept as best available description of the plausible vegetation of an area, we simulated PNV for the second half of the Holocene (6200 CE) using the CARbon Assimilation In the Biosphere (CARAIB) dynamical vegetation model (Dury et al., 2011; François et al., 2011; Laurent et al.,

2008; Otto et al., 2002; Warnant et al., 1994), forced by downscaled bias-corrected climate simulated by the iLOVECLIM model (Zapolska et al., 2023).

### 2.2. Design of the climate simulations

The climate simulations were performed with the iLOVECLIM model, version 1.1.5 (revision 1512). This model is a code fork of the original LOVECLIM 1.2 model (Goosse et al., 2010), revised by Roche (2013) and further expanded by Quiquet et al. (2018). In this study we used the online interactive downscaling method embedded in iLOVECLIM, first described by Quiquet et al. (2018). Our version of iLOVECLIM includes the following components: the atmospheric model, ECBilt (Opsteegh et al., 1998), the sea-ice ocean component, CLIO (Goosse and Fichefet, 1999), and the reduced-form dynamic global vegetation model, VECODE (Brovkin et al., 1997). We refer the reader to the reference articles for a complete description of the iLOVECLIM model (Roche, 2013) and downscaling method (Quiquet et al., 2018; Arthur et al., 2022).

Vegetation is an important component of climate dynamics, which impacts climate via physiological, biogeophysical and biogeochemical processes. It is, therefore, necessary to simulate vegetation cover to accurately simulate climate. This is why our climate simulations were performed with the VECODE reduced-form vegetation model (Brovkin et al., 1997) which computes plant and soil behaviours necessary to simulate the first order vegetation-climate feedback in climate models. Being a reduced-form DGVM, VECODE only computes 2 vegetation types: trees and grass (and bare ground as a dummy type). This is enough for the first order feedback to the atmospheric model, since it encompasses the three main classes affecting the albedo, the surface roughness and the link to the water cycle. However, it is far from being sufficient to reflect vegetation changes at the level of complexity needed for our main intercomparison with the REVEALS output, as described further in this study. This is why the resulting climatic evolution was then bias-corrected and used as an input to a much more complex vegetation model which has the necessary complexity to see the fine-scale structures we are concentrating on. The input was provided as climatologies (climatological means) of daily values for each time window (TW) (Supplementary Table 1) without transient change in climate input (equilibrium simulations). To summarise, the use of VECODE in the initial computation affected the large-scale climate providing the first-order response of dynamical vegetation coupled to climate at large scales, such as desertification (complete change from trees to grass or bare ground, and vice versa) or large shifts from forests to grassland. Fine-scale changes were then computed using the more complex (and more computationally intensive) CARAIB DGVM, so as to look into changes that are usually attributed to human impact on vegetation, such as changes in vegetation composition which are far beyond the reach of the reduced-form VECODE model. The coherency of the large-scale changes of the two vegetation models has been checked through the intercomparison between the results of the two models, and the results showed that they are consistent in patterns of large-scale vegetation response to climatic factors (not shown).

We applied iLOVECLIM to simulate the transient evolution of the climate during the Holocene. The experiments were first initialised with a state derived from a 3000 year long equilibrium simulation at 11,700 BP. Subsequently, we performed a full transient simulation from 11,700 BP up to present. Owing to the large time scale response of the ocean and furthermore to the fact that the climate system is never in equilibrium with forcing boundary conditions, we only considered the part 6000 BP to present in our analysis, using section 11,700 BP to 6000 BP as a further adaptation of climate to transient boundary conditions. For both equilibrium and transient simulations, we used boundary conditions evolving as closely as possible to the state of knowledge. Namely, we used astronomical parameters from Berger (1978), greenhouse gas levels (Schilt et al., 2010; Raynaud et al., 2000), ice sheets from the



GLAC-1D reconstruction (Tarasov et al., 2012; Tarasov and Peltier, 2002) as well as evolving bathymetry and land-ocean mask coherent with those ice-sheet geometries (with the same methodology as Bouttes et al., 2023). Between the year 6200 BP and the year 700 BP time windows (TWs) (Supplementary Table 1) were assigned at 500 years temporal resolution, and the lengths of the three most recent time windows were fixed to 350 (700–350 BP), 250 (350–100 BP), and 165 (2015 CE–1850).

The use of the model results for the intercomparison with pollen data in the context of the current study could be considered indicative under assumption of minimal model biases. To correct biases of iLOVECLIM modelled results, we applied the CDF-t bias correction technique (Vrac et al., 2012). CDF-t was previously reported to yield significantly stronger agreement between the simulated results and pollen-based climate and biome reconstructions, compared to modelled results without CDF-t application (Zapolska et al., 2023). A full procedure of the bias correction methodology and its limitations can be found in Zapolska et al. (2023).

The observational reference dataset used for bias correction is the EWEMBI dataset (Earth2Observe, WATCH Forcing Data (WFDEI), and ERA-Interim reanalysis data merged and bias-corrected for the Inter-Sectoral Impact Model Intercomparison Project) (Lange, 2016). The EWEMBI data covers 38 years from 1979 to 2016. To match to the length of the observation dataset (which is required for the CDF-t methodology), we extracted 38 median years of 14 TWs (Supplementary Table 1), consistent with the TWs of the REVEALS pollen-based land-cover reconstruction dataset for further analysis. Following the bias correction, each of 14 sets of climatic parameters was averaged to get daily mean climate characteristics of TWs.

The reliability of the described modelling workflow and the comparison of simulated climate and vegetation with available proxy data were evaluated in previous studies. Arthur et al. (2022) assessed the downscaled iLOVECLIM simulation for the Holocene before the application of CDF-t, while Zapolska et al. (2023) evaluated the downscaled iLOVECLIM and CARAIB performance for periods characterized by different climatic conditions with the CDF-t application.

### 2.3. Modelled potential natural vegetation

Potential natural vegetation was simulated using the CARbon Assimilation In the Biosphere (CARAIB) model (Otto et al., 2002; Laurent et al., 2008; Warnant et al., 1994; François et al., 2011; Dury et al., 2011) forced with 14 sets of climates simulated by the iLOVECLIM model (bias-corrected and averaged over TWs, as described above). The CARAIB model is composed of five modules describing respectively (1) the hydrological budget, (2) canopy photosynthesis and stomatal regulation, (3) carbon allocation and plant growth, (4) heterotrophic respiration and litter/soil carbon dynamics, and (5) plant competition and biogeography (François et al., 2011). In this study, we did not include the fire module in the simulations, and the fire regime was calibrated based on modern times. Water and carbon reservoirs in CARAIB are updated with a daily timestep, while photosynthesis and plant respiration are calculated every 2 h to account for non-linear effects associated with the variation of photosynthetic/respiration fluxes over the day. The model simulates a given set of plant functional types (PFTs), which can coexist on the same grid cell. Trees are assumed to grow above herbs and shrubs (or bare ground), creating two vegetation levels with maximum coverage up to 1 at each level. Thus, the maximum vegetation fraction of a grid cell is 2, provided that both upper (trees) and lower (grass and shrubs) levels are fully vegetated. Vegetation cover output is updated every month for herbaceous PFTs and yearly for arboreal PFTs (François et al., 2011; Henrot et al., 2017). For a more detailed description of the CARAIB model we refer the reader to Otto et al. (2002), Laurent et al. (2008), Warnant et al. (1994), François et al. (2011), Dury et al. (2011).

The input climatic fields used to run the CARAIB vegetation model were daily values of: (1) the mean near-surface air temperature, (2) the

daily amplitude of air temperature change, (3) precipitation, (4) air relative humidity, (5) percentage of sunshine hours and (6) wind speed. In the current study, daily temperature amplitudes and wind speed were taken from observations (Daily temperature amplitudes: Climatic Research Unit (CRU) data, mean over 1901–2015; wind speed: EWEMBI dataset) and kept constant for all time periods. Surface temperature, precipitation, relative humidity, and sunshine hours were derived from iLOVECLIM. Biases in temperature, precipitation and relative humidity were corrected using the CDF-t approach (Vrac et al., 2012). These sets of bias-corrected climate data were used to perform snapshot simulations with CARAIB run until equilibrium (200 years), to obtain characteristic PNV patterns for the specified TWs.

### 2.4. The REVEALS pollen-based land-cover reconstructions

For comparison with the modelled PNV, we used a part of the last set of gridded pollen-based REVEALS plant-cover estimates for 31 taxa at a spatial scale of  $1^\circ \times 1^\circ$  across  $30^\circ\text{--}71^\circ$  N,  $20^\circ$  W– $47^\circ$  E (north-western, central Europe, Mediterranean area, and part of the East until  $47^\circ$  E) for 14 contiguous time slices of 100–500 years covering second half of the Holocene (Serge et al., 2023). Previous grid-based estimates (Githumbi et al., 2022; Trondman et al., 2015) were designed for the purpose of conducting studies on the impact of land cover on climate using climate models and DGVMs (Strandberg et al., 2022). The REVEALS dataset is the only current land-cover reconstruction approach based on pollen data to quantify past regional cover of individual plant taxa. It effectively accounts for intertaxonomic differences in pollen productivity and dispersal properties as well as the size and type of sedimentary basins. It combined 1607 pollen records and benefited from earlier efforts and projects (Landclim I and II) in collecting pollen dataset (Githumbi et al., 2022; Trondman et al., 2015) obtained from databases and individual data contributors. There are many areas of Europe where environments that preserve pollen (i.e. lakes, bogs, forest hollows) are sparse, therefore the geographic distribution of pollen-based reconstruction is uneven.

REVEALS transforms pollen assemblages in large lakes to abundance of individual plant taxa in the surrounding vegetation at a large spatial scale (ca.  $100\text{ km} \times 100\text{ km}$ ; Hellman et al., 2008a, b) using a mechanistic modelling approach that uses an empirical understanding of relative pollen production between pollen morphological types, and pollen dispersal mechanisms. It was developed for pollen records from large lakes (>50–100 ha), but extensive simulation and empirical studies showed that multiple small-sized sites can be used when large lakes are not available in a region, although it generally results in larger standard errors on the estimates of plant cover (Sugita, 2007; Fyfe et al., 2013; Mazier et al., 2012; Trondman et al., 2015). As previous studies (Mazier et al., 2012; Trondman et al., 2015; Githumbi et al., 2022), Serge et al. (2023) used a  $1^\circ$  resolution grid and applied REVEALS on all available pollen records in each grid cell to produce an estimate of plant taxa abundance per grid cell through time. The estimates obtained for 31 individual taxa were later summed to produce estimates of the area occupied by plant functional types according to Table 1. Estimating the proportion of bare ground using pollen reconstructions is challenging due to the inherent limitations of the data. Hence, in REVEALS data, the total cover of plant taxa within a grid cell is always 100%.

All gridded REVEALS reconstructions for Europe follow the same protocol and criteria as published in Mazier et al. (2012) and Trondman et al. (2015), and lately by Githumbi et al. (2022). Gridded REVEALS estimates are influenced by the quality of individual records used (pollen count size, taxonomic resolution, and chronological uncertainty), basin size, and type of sites (lakes or bogs), the number of pollen records used in each grid cell, and the reliability of the relative pollen productivities (RPPs) used (Githumbi et al., 2022; Trondman et al., 2015; Serge et al., 2023). The precision of gridded REVEALS estimates is indicated by their standard errors. Caution should be applied when using REVEALS estimates from unreliable grid cells, and when standard



**Table 1**

Plant-functional types and corresponding plant taxa according to previously published classification used for model–data comparison in palaeovegetation studies (François et al., 2011; Henrot et al., 2017; Popova et al., 2013).

CARAIB PFT	Short name	Plant taxa/pollen-morphological types (31 taxa)
Herbs (C3 herbs “humid”, C3 herbs “dry”, C4 herbs)	H	Amaranthaceae/Chenopodiaceae, <i>Artemisia</i> , Cerealia t., Cyperaceae, <i>Filipendula</i> , <i>Plantago lanceolata</i> , Poaceae, <i>Rumex acetosa</i> t., <i>Secale cereale</i>
Broadleaved evergreen boreal/temp cold shrubs	BEBTS	<i>Calluna vulgaris</i> , Ericaceae
Broadleaved evergreen temperate warm shrubs	BETWS	<i>Buxus sempervirens</i>
Needleleaved evergreen boreal/temp cold trees	NBTT	<i>Abies</i> , <i>Juniperus</i> , <i>Picea</i> , <i>Pinus</i>
Broadleaved evergreen meso-mediterranean trees	BEMMT	<i>Phillyrea</i> , evergreen <i>Quercus</i> t.
Broadleaved evergreen thermo-mediterranean trees	BETMT	<i>Pistacia</i>
Broadleaved summergreen boreal/temp cold trees	BSBTT	<i>Alnus</i> , <i>Betula</i> , <i>Corylus avellana</i> , <i>Salix</i>
Broadleaved summergreen temperate cool trees	BSTCT	<i>Carpinus betulus</i> , <i>Fagus</i> , <i>Fraxinus</i> , deciduous <i>Quercus</i> t., <i>Tilia</i> , <i>Ulmus</i>
Broadleaved summergreen temperate warm trees	BSTWT	<i>Castanea sativa</i> , <i>Carpinus orientalis</i> / <i>Ostrya</i> t.

errors of the gridded REVEALS estimates are equal or greater than REVEALS estimates (Serge et al., 2023). Hence, the number of available REVEALS grid cells for analysis varies depending on the availability of reliable pollen data for each TW. Across the 14 TWs studied here, the number of grid cells ranged from 456 to 363. This range reflects variations in quantity and quality of the pollen data available for analysis during each time window.

## 2.5. Classification of plant functional types

To reconstruct vegetation patterns and their changes throughout the Holocene we applied the concept of plant functional types (PFTs). Plants were classified into PFTs based on their physical, phylogenetic and phenological characteristics, as well as their bioclimatic and functional features. PFTs included in the CARAIB model are described in François et al. (1998). In this study, each selected plant taxon was assigned to a specific unique PFT (Table 1) based on previously published classification used for model–data comparison in palaeovegetation studies (François et al., 2011; Henrot et al., 2017; Popova et al., 2013). Standard errors of the REVEALS dataset (Serge, 2023) were calculated for each PFT according to the delta method (Stuart and Ord, 1994).

In CARAIB, plant growth in northern Europe is hindered by frigid climatic conditions of polar tundra, which prevents vegetation from populating the grid cells. Therefore, high latitudes in CARAIB are composed of bare ground with a few herbs (Supplementary Fig. 7). Pollen-based reconstructions, however, reflected presence of *Betula*, Ericaceae, Cyperaceae, *Pinus* and Poaceae in those areas across all studied TWs. A recent study of Sun et al. (2022) demonstrated the impact of the lack of representation of bare ground in REVEALS-based estimates. Hence, to eliminate some of the potential biases related to this issue, we chose to exclude high latitudes (70–71°N) from the intercomparison. With this we aimed to prevent the negative bias due to low agreement between the studied datasets over these zones, dictated by their technical characteristics. Furthermore, it is important for readers to exercise caution when interpreting regions with a high fraction of bare ground in the CARAIB model outputs (e.g., certain parts of the Iberian Peninsula) (Supplementary Fig. 7). The differences in the representation of bare ground across the studied datasets may increase the uncertainty of the analysis in these areas.

## 2.6. Comparison between REVEALS estimates and CARAIB simulations

Comparison of the CARAIB simulations with the REVEALS estimates required a transformation of the spatial and temporal resolution of the CARAIB model output. We aggregated the PNV simulated by CARAIB to the same grid resolution as the REVEALS estimates (1°x1° grid cells) and extracted only those grid cells where the pollen data were available (ranging from 456 to 363 grid cells for the analysed TWs). CARAIB vegetation is represented by two vertical layers that were adjusted to match a resolution of 1°, used by the REVEALS method.

Then, relationship between REVEALS and CARAIB was analysed by computing a weighted matching ratio between PFT fractions of both models, using the following formulas:

$$MR_{PFT} = \frac{frac_{PFT, reveals}}{frac_{PFT, caraib}} \times 100,$$

and

$$WMR = \sum_{PFT=1}^{Nb_{PFT}} \frac{frac_{PFT, reveals}}{frac_{PFT, reveals}} \times MR_{PFT},$$

where Nb. PFT – maximum number of PFTs,  $frac_{PFT, reveals}$  – fraction of a PFT in REVEALS dataset,  $frac_{PFT, caraib}$  – fraction of corresponding PFT in CARAIB dataset,  $MR_{PFT}$  – matching ratio per PFT, WMR – weighted matching ratio of REVEALS and CARAIB.

Similarity between CARAIB and REVEALS estimates per PFT was expressed in matching ratio (MR) values. Considering that the two datasets are independent and of a different nature, the use of absolute values of MRs for the intercomparison could have been challenging due to limitations and biases of the methodology. Such biases remain in all TWs (assuming their stationarity), but MRs may not be constant through time. In this study it is assumed that this variation occurs due to human impact, which is the factor that is not stationary in time throughout our study period. Therefore, we focused on temporal changes within PFTs rather than absolute differences between the datasets to minimize the impact of such biases on our results. To this end, we have chosen to analyse the relative change in the MR values between each TW and the TW calculated in the most recent period (TW1).

WMR was calculated to ensure that more weights are given to the PFTs that are more abundant within a grid cell. Under an assumption that WMR represents percentage of vegetation unaltered by anthropogenic activity, by reversing it we calculate a human pressure index (HPI):

$$HPI = (100 - WMR) \div 100.$$

Then, a mean HPI over each 1°-wide latitudinal zone was calculated for each TW.

Translating the discrepancies between the two studied datasets into the HPI was made under the assumption that changes in relationship between the two datasets at the second half of the Holocene are mainly caused by anthropogenic activity. This assumption is supported by a growing body of evidence, including palaeoenvironmental reconstructions, that suggests a significant and widespread impact of human activities on European land-cover during this period (Roberts et al., 2018, 2019; Ruddiman and Ellis, 2009; Nielsen et al., 2012; Kaplan et al., 2009; Ellis et al., 2013; Strandberg et al., 2022). While megafauna presence is also not simulated by PNV models, the extinction of many megafaunal species during the late Pleistocene and the Holocene in Europe (Mann et al., 2019; Sandom et al., 2014; Stewart et al., 2021; Koch and Barnosky, 2006) decreases their potential role in large-scale changes in vegetation patterns over the second half of the Holocene. Taken together, these lines of evidence support our assumption that anthropogenic activity is the main driver of changes in the relationship between the datasets during the second half of the Holocene.

2.7. Correlation with ALCC scenarios

In order to compare our results with existing literature on anthropogenic impact on European land-cover, we used two most commonly used in landscape research ALCC scenarios, KK10 and HYDE 3.2. ALCCs offer the advantage over other datasets as they provide datasets that are continuous in space and time, whilst other approaches (for example, demographic proxies such as archaeological dates (e.g. Shennan et al., 2013), or human impact indicators from pollen data) have discontinuous coverage, and are not necessarily linearly related to land cover changes (Hiscock and Attenbrow, 2016). KK10 and HYDE 3.2 differ in the way they estimate and represent land-cover change. KK10 consists of data expressed in a form of a deforestation index at annual resolution, which, in this study, was averaged over the years within each of the REVEALS time windows (Supplementary Table 1). HYDE 3.2 estimates are presented in a form of simulated land use. In this study, to represent anthropogenic land use for agricultural purposes we analysed HYDE 3.2 data on croplands and grazing. HYDE 3.2 data is irregularly spaced in time over the Holocene: from 100 years temporal resolution in the Late Holocene to 1000 years in the early and Mid-Holocene. We used linear interpolation to obtain the data for the studied time windows. We also performed transformations of spatial resolution of both ALCC scenarios by aggregating the grid cells to the 1°x1° REVEALS grid, and extracted data only for the grid cells that have available data in REVEALS.

For comparison between HPI and KK10 and HYDE, we assumed that extracted land use from the ALCC scenarios should be roughly equivalent to human impact on land-cover. We then analysed correlation between these three datasets to investigate if they represent human-induced land-cover changes in a similar manner. Additionally, we evaluated the relationship between HPI values and HYDE 3.2 population density estimates to understand if presence of humans spatially correlates with changes in HPI. HYDE 3.2 population density is primarily based on demographers' estimates for the last 3000 years (McEvedy and Jones, 1978), with earlier population sizes being estimated using back extrapolation (Goldewijk et al., 2010).

3. Results

We have analysed palaeovegetation data expressed in fractions of PFTs for 14 TWs throughout the second half of the Holocene (6200 CE) from CARAIB simulations (representing PNV) and REVEALS estimates (representing pollen-based regional vegetation abundance). The definitions of TWs are summarised in Supplementary Table 1.

The analysis of the relationship between simulated PNV and pollen-based regional estimates of vegetation abundance is based on the evolution of discrepancies in the two datasets and expressed as relative change in the MR values between each TW and the TW calculated in the most recent period (TW1) (Fig. 1). Throughout the studied time period, we observe decreases in MR of herbs (H), broadleaved summergreen boreal/temperate cold trees (BSBTT) and broadleaved summergreen temperate cool trees (BSTCT). MR of broadleaved evergreen boreal/temperate cold shrubs (BEBTS) increases, and MR of broadleaved evergreen temperate warm shrubs follows a non-linear trend.

Fig. 1 shows that different PFTs had different levels of dissimilarities and evolved differently through time. Therefore, to analyse anthropogenic impact on vegetation dynamics that would account for all the changes within PFTs we introduce a human pressure index (HPI). HPI is calculated based on matching ratios of individual PFTs for each grid cell, and the weight of the variables is determined by the abundance of each PFT in the REVEALS estimates.

We observe high HPI values at 5700–6200 BP (TW14) across the Mediterranean region and eastern Europe (Fig. 2). Throughout the Holocene HPI values become progressively higher in central, western and northern Europe, with the majority of the grid cells having extremely high HPI values at modern time (TW1) across the continent. During the whole studied period high HPI is observed in northern Europe (Scandinavia), which is an artefact of intrinsic biases of two datasets compared (Section 4.4). Hence, the high latitudinal zones (70–71°N) are not included in the subsequent analyses.

In Fig. 3, we subdivide our study area into latitudinal zones of 1°, corresponding to the size of grid cells used for our analysis. This division allows us to display latitudinal trends of HPI changes through the second half of the Holocene in Europe. We chose to present the dynamic per latitudinal zone based on the historical context of our study period in

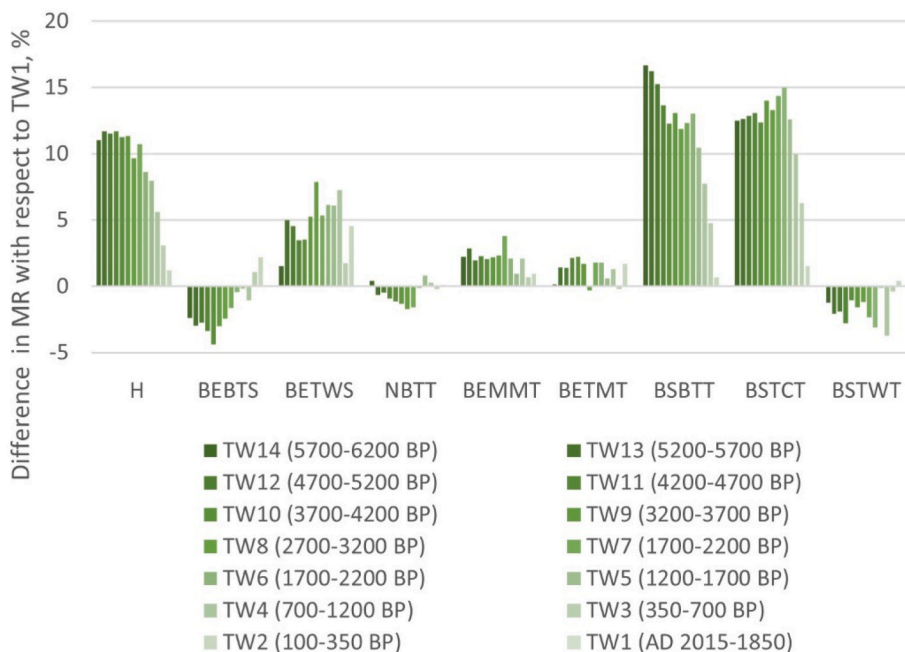


Fig. 1. Temporal evolution of agreement per PFT between the CARAIB simulations and the REVEALS estimates expressed as difference in matching ratio (MR) from MR at TW1 (present - 100 BP).



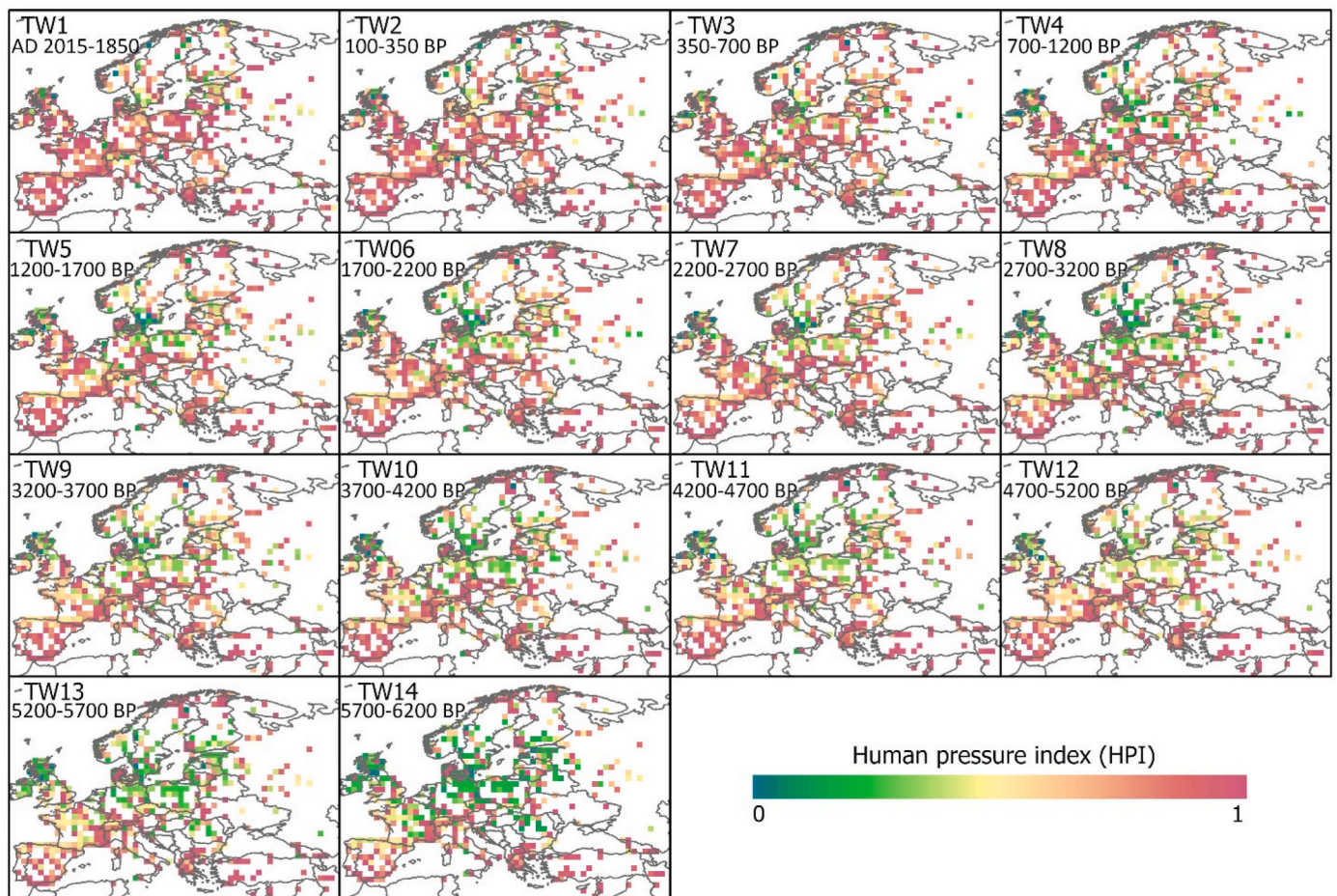


Fig. 2. Human pressure index per grid cell in Europe from TW14 (5700–6200 BP) to TW1 (present - 100 BP). 1-Highest human pressure; and 0-lowest human pressure value.

Europe, which corresponds to the transition and establishment of agriculture (Stephens et al., 2019; Morrison et al., 2021; Harrison et al., 2020; Goldewijk et al., 2017a; Kaplan et al., 2011; Gronenborn and Horejs, 2021). Archaeological sources (e.g. Gronenborn and Horejs, 2021; Stephens et al., 2019) provide evidence that this agricultural transition followed a south-to-north trend, with agriculture being established first in the Mediterranean region, and gradually expanding northward. While we acknowledge that this is an oversimplified description of the complex dynamics of the processes involved, by presenting the data in this manner, we visualize the general temporal trend of HPI increase, potentially largely affected by the agricultural expansion.

Vegetation of mid-latitudes resulted to be relatively preserved at earlier times. Contrastingly, Southern latitudes (37.5°N to 41.5°N) have relatively high HPI throughout the studied period. 42.5°N to 54.5°N are the areas where the changes are the largest within the studied time-frame, demonstrating a northward direction of HPI increase in time through the second half of the Holocene.

Although there are limitations to the methodology used in our study that affect the robustness of our results in northern latitudes, we observe a clear and gradual increase in HPI over time at latitudes south of 54.5°N (Fig. 3), which covers a large part of continental Europe. This enables us to track the long-term dynamics of human activity on land-cover across both time and space for a significant portion of the continent, which is where the majority of vegetation changes have occurred.

To determine statistical significance of our results, and their evolution in comparison to present day, we calculate the percentage of grid cells with HPI values significantly different from the modern time TW1

at the 0.05 level (paired Student's t-tests). Fig. 4 illustrates that the percentage of grid cells with values that indicate significantly lower human pressure compared to modern values (N–S) decreases as we move from early time to modern time, indicating that roughly 60% of grid cells had significantly lower HPI (are significantly less impacted by human activity) at 5700–6200 BP, compared to modern values.

Overall, across Europe our results indicate a gradual increase of HPI throughout the second half of the Holocene (Fig. 5), which escalated after TW5 (1200–1700 BP). Moreover, at the beginning of our simulation (TW14) we observe an average HPI of 0.72, which suggests that vegetation cover in Europe at 5700–6200 BP corresponded to modelled potential natural state of vegetation only for nearly 30%.

Re-analysis of the KK10 and HYDE 3.2 estimates at REVEALS spatio-temporal resolution reveals that HYDE 3.2 cropland and grazing area increase (Fig. 6, left), and KK10 deforestation for agriculture rise (Fig. 6, right) follow similar patterns to HPI increase (Fig. 5). However, the initial HPI values at TW14 are significantly higher than anthropogenic land use change compared to the rates of spread of agricultural practices (Supplementary Figs. 3 and 4).

To further investigate the relationship between HPI and agriculture, we analyse the onset of agriculture in REVEALS vegetation reconstructions, marked by first appearance of *Cerealia* t. And *Secale cereale* pollen in the dataset. We assume that the agricultural onset is represented as a year of the earliest (within the time bounds of our study) appearance of the aforementioned agricultural taxa in REVEALS at each grid cell (Supplementary Fig. 6). However, the identification of the onset of agriculture based on agricultural PFT in REVEALS is constrained by the limitations of this approach, described by Trondman



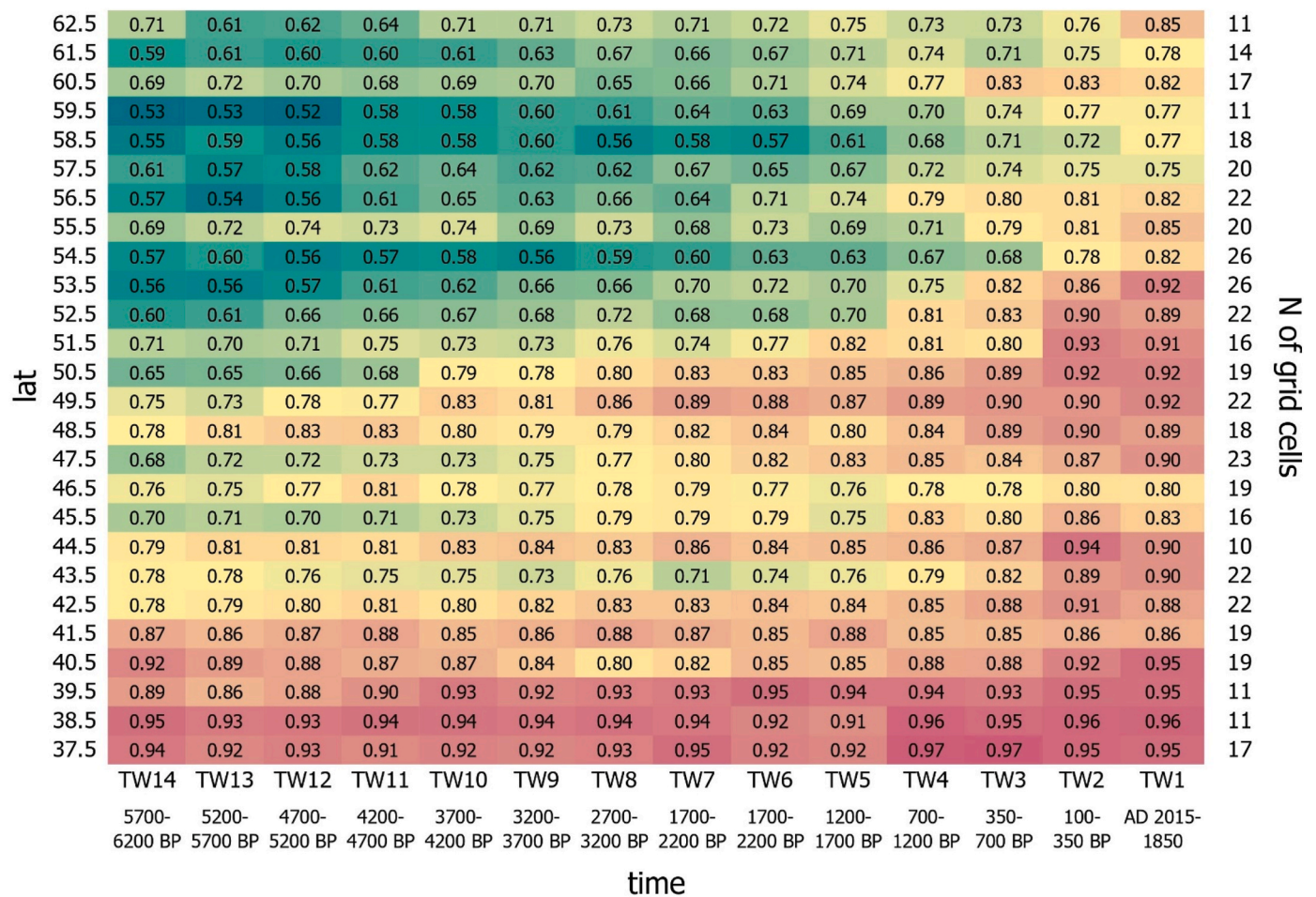


Fig. 3. Human pressure index (HPI) over latitudinal zones in Europe from TW14 (5700–6200 BP) to TW1 (present - 100 BP). 1-Highest human pressure; and 0-lowest human pressure value. Zones with less than 10 grid cells are not shown.

et al. (2015). We, therefore, do not identify patterns similar to the onset of agriculture in Europe described by the existing anthropogenic land-cover change (ALCC) scenarios.

Additionally, we explore the correlation between HPI and ALCC simulated agricultural practices. Although we observe a weak correlation between the two variables (Supplementary Figs. 3–4), the HPI index at 5700–6200 BP is significantly correlated with HYDE 3.2 population density estimates (Fig. 7), thus reflecting human presence in landscapes.

#### 4. Discussion

Analysing land-cover change in Europe using REVEALS estimates and independent climatic and land use data, Marquer et al. (2017) suggested that climate is a major driver of vegetation change during the Holocene as a whole and at the sub-continental scale, stating that the land use impact increase gradually after 7000 BP while identifying four critical phases of land use effects on vegetation. Our methodology compared REVEALS estimates with simulated climate-only-driven potential natural vegetation (PNV) over the studied period to discount from the analysis changes in vegetation that were predominantly caused by changing climate. Previous studies suggest that climate change and anthropogenic activity are assumed to be the main driving factors of land-cover change in Europe over the second half of the Holocene (Marquer et al., 2017; Strandberg et al., 2022; O’Dwyer et al., 2021; Kuosmanen et al., 2018; Poska et al., 2022; Roberts et al., 2019, 2018). Thus, the difference between the two types of vegetation was introduced as a human pressure index (HPI). This index represents how different reconstructed vegetation is from a natural state, and thus includes both

direct (i.e. deforestation and plant cultivation) and indirect (through biogeochemical feedbacks) anthropogenic changes in vegetation composition. These changes reflect continuous and prolonged human impact on European land-cover through various practices, which accumulated their consequence over time, building up a cumulative human pressure.

##### 4.1. Fire regime

In this study, CARAIB simulations did not include the fire module, and thus, the potential impact of wildfires could contribute to dissimilarities between PNV and vegetation reconstructions. The studied period in Europe is covering a transition from hunter-gatherer to agricultural societies (Stephens et al., 2019; Gronenborn and Horejs, 2021). Human induced biomass burning was previously linked to both agricultural (i.e. slash-and-burn) (Vannière et al., 2016) and non-agricultural practices (i.e. initiating selectively support food growth, tool in social interactions, or keeping away predators) (Scherjon et al., 2015). Thus, fires throughout the studied period were expected to have predominantly anthropogenic origin, which reflects human pressure on land-cover, and thus contributes to increase in HPI. Previously, sedimentary charcoal composites analysis revealed that humans have significantly influenced fire activity throughout the Holocene in Europe (Dietze et al., 2018; Connor et al., 2019; Vannière et al., 2016; Carracedo et al., 2018), and outlined that human impact on fire regime could be both direct (via its use as a land management tool) and indirect (via affecting biogeochemical cycles and increase landscape flammability) (Dietze et al., 2018; Connor et al., 2019). Thus, the wildfire regime of the studied

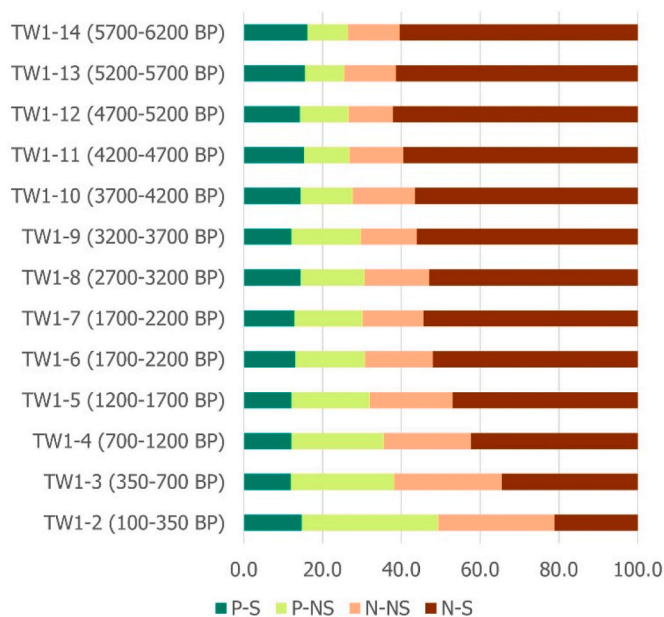


**Fig. 4.** Percentage of grid cells with indicated difference in HPI between the TW1 (2015–1850 CE) and each consequent TW. P: positive slope (the most recent time window has lower human pressure index); N: negative slope (the most recent time window has higher human pressure index); S: significant; NS: non-significant at the 0.05 level (paired Student's t-tests). For example, for the difference between TW14 and TW1, the dark brown part of the bar shows that 60% had a statistically significant negative slope, indicating that TW1 had a significantly higher HPI value than TW14. For the maps of the differences in HPI please refer to the [Supplementary Figs. 1 and 2](#).

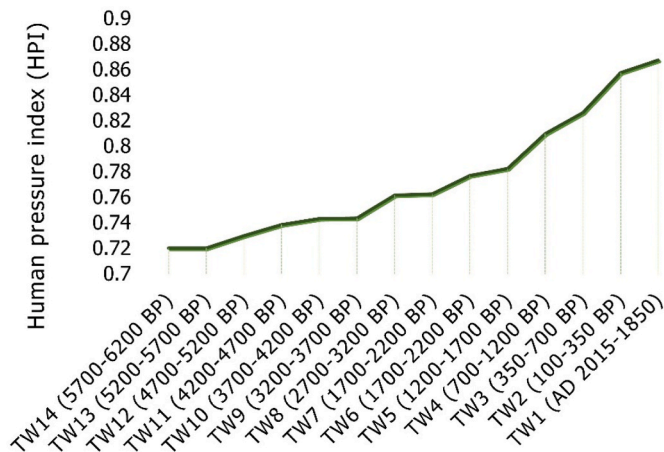


**Fig. 5.** Human pressure index (HPI) in Europe from TW14 (5700–6200 BP) to TW1 (present - 100 BP).

period was also altered by human activities, which brings additional challenges to making a clear distinction between “natural” and “anthropogenic” fires (e.g. [Vanni re et al., 2016](#); [Power et al., 2008](#)). Due to not having available methods to separate natural from human-induced fires, and assuming minor role of natural fires in the analysis compared to anthropogenic impact on land-cover change, wildfires were not explicitly included in our analysis.

#### 4.2. Insight from REVEALS dataset analysis - comparison with previous studies

Previously, land-cover naturalness and anthropogenic impact on vegetation were assessed through analysing changes in forested areas

([Strona et al., 2016](#); [Kaplan et al., 2017](#); [Pirzamanbein and Lindstr m, 2022](#); [Woodbridge et al., 2018](#)) and via cultural indicator-types in pollen sequences ([Deza-Araujo et al., 2020, 2022](#); [Behre, 1981](#); [Mercuri et al., 2013](#); [Gaillard, 2013](#)). Apart from known cultivars, many cultural indicator pollen types are components of natural vegetation, characteristic of open conditions, natural grazing dynamics or disturbed soils, particularly in southern Europe ([Fyfe et al., 2019](#); [Roberts et al., 2019](#)) and thus require careful interpretation. Within the framework of the LANDCLIM project ([Gaillard et al., 2010](#)) anthropogenic land-cover changes were commonly expressed as vegetation openness indicated in the REVEALS model results ([Trondman et al., 2015](#)).

Recently, REVEALS estimates were compared with DVM-simulated vegetation with a goal of assessing land-cover change in Europe and analysing underlying processes behind the observed changes ([Dallmeyer et al., 2023](#)). Similar to our study, [Dallmeyer et al. \(2023\)](#) attributed varying discrepancy over time between the two datasets to human activity. Here we applied a more complex approach that takes into account vegetation composition in the form of fractions of plant functional types (PFTs) and their evolution through time, and used more spatially explicit REVEALS estimates. We identified that in addition to vegetation openness (expressed as fraction of herbaceous cover), anthropogenic changes affected distribution of other PFTs, such as broadleaved summergreen boreal/temperate cold trees (BSBTT), broadleaved evergreen temperate cool trees (BSTCT), broadleaved evergreen boreal/temperate cold shrubs (BEETS), and broadleaved evergreen temperate warm shrubs (BETWS) ([Fig. 1](#)). [Lechterbeck et al. \(2014\)](#) also found that early agriculture resulted in compositional changes in forests in southern Germany, rather than increased openness.

Analysing the REVEALS dataset, [Marquer et al. \(2017\)](#) indicated a decrease of broadleaved forest and an expansion of coniferous woodland during the Mid-Holocene. Our findings support the hypothesis about the anthropogenic nature of changes in broadleaved summergreen PFTs (BSBTT and BSTCT) ([Fig. 1](#)). However, contrastingly to [Marquer et al. \(2017\)](#), we observed no significant variation in MR of needleleaved evergreen plant group (NBTT), which suggests that the coniferous woodland expansion reported by [Marquer et al. \(2017\)](#) is likely driven by climatic factors. In addition to changes in vegetation openness and herbs (such as *Filipendula*, *Artemisia*, *Plantago* and *Rumex acetosa* t.) ([Gaillard, 2007](#)), anthropogenic activity in REVEALS estimates were previously attributed to changes in agricultural taxa (*Cerealia* t. And *Secale cereale*) ([Trondman et al., 2015](#)). Our results supported the hypothesis about anthropogenic nature of changes in openness, represented by the fraction of herbs. However, we observed the absence of statistically significant difference in HPI values between grid cells with and without the presence of agricultural taxa in REVEALS ([Supplementary Fig. 5](#)). The observed results may be attributed to the representation of agricultural land in REVEALS reconstructions. For example, the classification does not include other cultivated plants, such as *Fagopyrum* (buckwheat), *Linum usitatissimum* (common flax) and *Juglans regia* (walnut) ([Trondman et al., 2015](#)). This suggests that the HPI reflects human pressure on vegetation in a more broad sense than just *Cerealia* t. And *Secale cereale* crop cultivation.

#### 4.3. Consistency of our findings with ALCC scenarios

Contrastingly, the evolution of HPI patterns through the studied period generally coincide in time and location with previously simulated by ALCC human induced vegetation changes. Anthropogenic impact on land-cover was previously reported to shift north throughout the second half of the Holocene ([Goldewijk et al., 2017a](#); [Kaplan and Krumhardt, 2011](#); [Stephens et al., 2019](#)), which is reflected in HPI values, which rise following similar trajectory ([Fig. 3](#)). Moreover, at 6000 BP our results present a general agreement in patterns of HPI with the KK10 ALCC scenario ([Kaplan and Krumhardt, 2011](#)). Both indicate anthropogenic land-cover modifications across Mediterranean Europe and partial modifications in central and northern Europe ([Fig. 2, Supplementary](#)



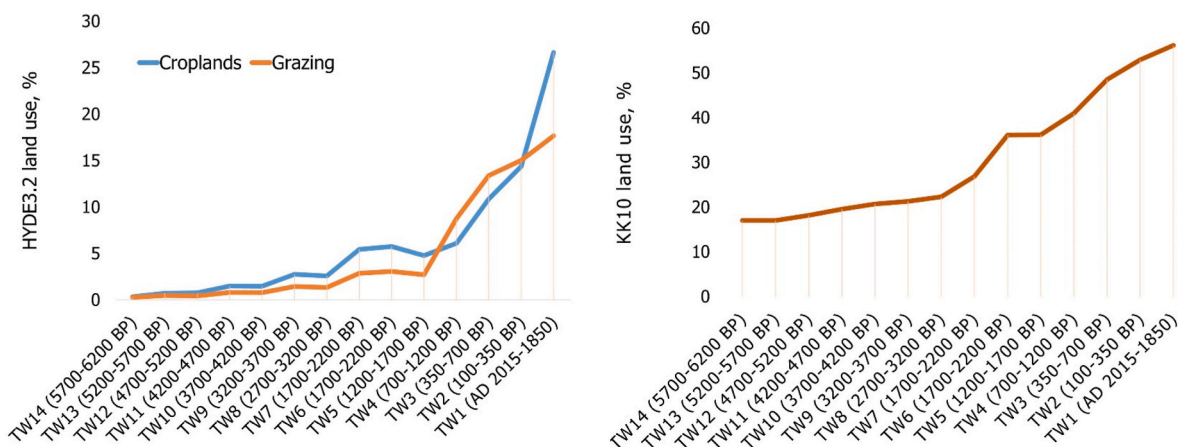


Fig. 6. HYDE 3.2 simulated land use, expressed as fraction of croplands and grazing per grid cell (left panel), and KK10 simulated land use, expressed as deforestation index (right panel).

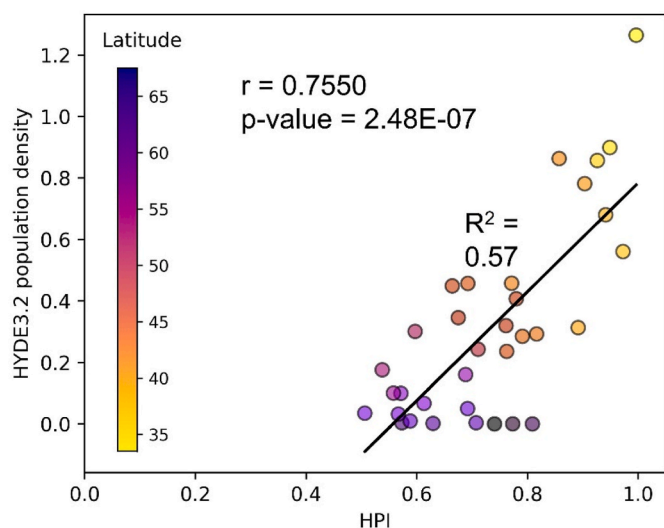


Fig. 7. Correlation between human pressure index (HPI) versus HYDE 3.2 population density estimates over latitudinal zones in Europe for TW14 (5700–6200 BP).

Fig. 1). The areas of high human pressure index coincide with the spread of agriculture, indicated in the HYDE 3.2 ALCC (Goldewijk et al., 2017a). However, HPI indicated higher anthropogenic land-cover change at 6000 BP than KK10 and HYDE 3.2 in eastern Europe, which is not reflected in either of the two ALCC. It should be noted that both ALCC scenarios are derived from GIS models that are primarily based on population estimates and geographic information (Marquer et al., 2017; Kaplan et al., 2009; Goldewijk et al., 2017a). Therefore, they are constrained by various methodology limitations and do not always agree with archaeological records. For example, findings of KK10 and HYDE 3.2 scenarios for eastern Europe differ from conclusions of the ArchaeoGLOBE project, an empirical global assessment initiative of land use based on archaeological knowledge (Stephens et al., 2019). ArchaeoGLOBE results suggested that the onset of intensive (in the case of HYDE 3.2) and widespread agriculture (in the case of both KK10 and HYDE 3.2) in the region was significantly underestimated (for up to 7500 years) in both ALCC scenarios. According to ArchaeoGLOBE estimates, common levels of intensive agriculture onset in the region were present at 6000 BP (Stephens et al., 2019), which supported our results, indicating relatively high HPI values over the region in the Mid-Holocene (Fig. 2).

In our findings, we observed nearly 60% of grid cells to have a

significant increase in HPI values at TW1 (1850 CE–2005), compared to TW14 (5700–6200 BP) (Fig. 4). Since this period is characterized by the onset and spread of agriculture over the study region (Stephens et al., 2019; Kaplan and Krumhardt, 2011; Goldewijk et al., 2017a), we assumed this value to be largely attributed to agricultural activity. Reported increase in HPI agrees with the ALCC estimates and FAO land use statistics (FAO, 2022), which reports that 52.3% of the area of European Union was 1961 classified as agricultural. Similarly, the ALCC scenarios suggest that for the study area at TW1 (modern time) nearly 56% of land-cover was transformed by anthropogenic activity accordingly to KK10, and HYDE 3.2 estimates suggested nearly 45% of land-cover to be impacted by agriculture (18% grazing and 27% cropland) (Fig. 6). ALCC estimates agree with the FAO land use statistics (FAO, 2022), since they are partially based on FAO statistics (in case of HYDE 3.2). In this study we analysed data for continental Europe, contrastingly to FAO land use statistics, which is constrained by the EU borders. Additionally, the REVEALS dataset is not spatially continuous. Thus, the values in Fig. 6 are not directly comparable to FAO statistics. However, the ALCC land use indices at TW1 have similar levels of magnitude to extent of agricultural land reported by FAO, confirming that both KK10 and HYDE 3.2 mainly represent land-cover change for agricultural purposes, and indicating that the HPI detected land-cover change for agricultural purposes in a similar manner to analysed ALCC scenarios.

We note that agriculture appeared in Europe as early as ca. 8000–9000 BP (Stephens et al., 2019; Gronenborn and Horejs, 2021), and by the earliest TW covered in this study (5700–6200 BP), it had become widespread in some European regions (Stephens et al., 2019). Consequently, high HPI values at that period are to a degree attributed to early agricultural practices, particularly in the Mediterranean region and Southern Europe (Figs. 2 and 3). However, HPI shows a significantly larger anthropogenic land-cover change at TW14 (5700–6200 BP) than the two considered ALCCs (Figs. 5 and 6 Supplementary Figs. 3 and 4). Considering the fact that land-cover changes in KK10 and HYDE 3.2 reflect the establishment of the first agricultural societies (Goldewijk et al., 2017b; Kaplan et al., 2009), and show 17% and 0% of agriculture-driven landscape changes at TW14 correspondingly (Fig. 6), we suggest that high HPI values at TW14 (Figs. 3 and 5) are partially attributed to pre-agricultural anthropogenic land-cover modifications that accumulated throughout the history of human-environment interactions in Europe and led to high levels of vegetation divergence from potential natural state. These findings emphasize the importance of accounting for early anthropogenic landscape impact, reported in previous studies (Archibald et al., 2012; Bos and Urz, 2003; Doughty, 2013; McWethy et al., 2010; Pinter et al., 2011; Roberts et al., 2021; Ellis et al., 2021; Nikulina et al., 2022).



#### 4.4. Methodological limitations

It should be noted that the overestimation in HPI could be partially attributed to methodology limitations. Such limitations were caused by data availability in the REVEALS dataset, as well as by unequal reliability of the REVEALS grid cells (Serge et al., 2023). The intercomparison between reconstructed and modelled vegetation was also previously reported to be challenging (Dallmeyer et al., 2023). In addition, to correct biases of the used climate model we used the CDF-t approach (Vrac, 2018; Zapolska et al., 2023), but no bias correction was performed for the vegetation model (CARAIB). For the intercomparison PNV data was resampled and reclassified to be compatible with the REVEALS dataset, which in turn led to simplifications and resampling biases. For example, as in this work we assigned each taxon to a unique PFT category, the taxon Ericaceae was only included in broadleaved evergreen boreal/temperate cold shrubs (BEBTS) PFT (Table 1). However the Ericaceae family includes species that live both in the north and at high elevations (herbs and low shrubs, i.e. *Vaccinium*, *Arctostaphylos uva-ursi*), and in the South (trees, i.e. *Arbutus unedo*, *Erica arborea*) (Serge et al., 2023).

We hypothesise that the descending temporal trend and high HPI values in northern latitudes were mainly caused by the aforementioned methodology biases, such as PFT classification limitations and differences in representation of bare ground in studied datasets. Moreover, the trees at high latitudes might be confined in small topographic depressions that induce a local micro-climate that we cannot reproduce at our spatial scale. However, the rising HPI values through the studied period in most of continental Europe (south of 54.5°N) were mainly associated with human activity, which was previously reported to shift north throughout the second half of the Holocene (Goldewijk et al., 2017a; Kaplan and Krumhardt, 2011; Stephens et al., 2019).

#### 4.5. Quantifying uncertainties

It should be noted that the absolute HPI values (Figs. 2, 3 and 5) should be treated with caution, as they are affected by various methodology biases discussed in this study. To our knowledge, there is no approach to quantify given uncertainties. However, the study of Zapolska et al. (2023) estimated methodological uncertainties of the used approach by comparing PNV simulations from bias-corrected CARAIB and statistically modelled PNV distribution of Levavasseur et al. (2012), based on BIOME6000 pollen reconstructions. Their findings indicate that methodological biases can constitute up to nearly 50% when analysing matching ratios between PNV datasets of a different origin, which would place a lower boundary on the HPI absolute value at 6000 BP (Fig. 5) at about 30%, but likely more if median taken. To eliminate the impact of these biases on our conclusions, we emphasize the importance of changes from one TW to another, rather than absolute differences between the datasets, as the impact of methodology biases remains constant in all TWs (assuming their stationarity). Hence, our conclusions are largely based on the analysis of temporal changes in HPI values and trends that appear in these changes.

To verify our findings, further studies aimed at evaluation of human pressure on land-cover could compare the results using several vegetation models (i.e. Dallmeyer et al., 2023), undertake a detailed intercomparison with established and emerging pollen-indicator type approaches (e.g. Deza-Araujo et al., 2022), draw on more extensive compilations of pollen records, as well as investigate potential impact of bare ground in pollen-based reconstructions (e.g. through the application of the Modern Analogue Technique demonstrated by Sun et al., 2022). In addition, incorporating ALCC estimates in the workflow and introducing plant consumption by megafauna would allow further analysis of underlying processes behind detected land-cover changes.

#### 4.6. More than agriculture – pre-agricultural practices and land-cover naturalness

Despite the limitations of our study, the significant relationship between the HPI and HYDE 3.2 population density (Fig. 7) supported the suggestion that relatively high HPI values in the Mid-Holocene were mainly attributed to human vegetation cover modifications by the means of early agricultural and non-agricultural practices during the periods preceding TW14 (5700–6200 BP). It should be noted that HYDE 3.2 population estimates are highly debated in the land use community due to their uncertainties related to strong dependency on a few historical population sources, such as McEvedy and Jones (1978), Maddison (2001) and Livi-Bacci (2007) (uncertainty ranges reported by Goldewijk et al., 2017b). However, our conclusion on partially non-agricultural nature of high HPI values at Mid-Holocene is also supported by the widespread evidence of hunter-gatherer land use, which indicates that land-cover were largely transformed by humans prior to agricultural onset (Bos and Urz, 2003; Finsinger et al., 2006; Nikulina et al., 2022; Roebroeks et al., 2021; Scherjon et al., 2015). Moreover, findings of Ellis et al. (2021), based on the analysis of spatially explicit global reconstruction of historical human populations and land use, show that nearly three quarters of Earth's land was already inhabited by hunter-gatherer and/or early agricultural societies at the beginning of the current interglacial interval, transforming wildlands into cultured anthromes. Their conclusions are in line with our findings that indicate around 70% difference between reconstructed and potential natural state of land-cover at 5700–6200 BP (Fig. 5, TW14). Contrastingly, KK10 land use indicates 17% of land-cover change over the same study area at 5700–6200 BP (Fig. 6, right panel, TW14), which is rather an indicator for adoption of agriculture, than land-cover “naturalness”.

Notably, high HPI values at TW14 are concentrated in the Mediterranean region (see Fig. 2). In support of our findings, a synthesis of existing sedimentary charcoal records (Marlon et al., 2013) reports significant fire activity during the early Holocene in the same region. While the study of Marlon et al. (2013) acknowledges that it is challenging to analyse complex fire-vegetation-climate dynamics over the Mediterranean, they suggest strong dependence of the European early Holocene fire history on climate rather than human activity. Our findings, however, suggest a link between high early HPI and very high burning in the area during the early Holocene (~10,000 BP). It should be noted that Marlon et al. (2013) highlight the difficulty in establishing the link between temperature and human impact within each local sub-region. Additionally, even minor climate changes, such as slightly drier conditions, can facilitate human-triggered fires. Hence, we propose that climate change amplifies the dynamics of human-related fires, particularly in arid regions, as emphasized in the compilations of Marlon et al. (2013).

Nevertheless, HPI increase across the continent throughout our study period aligns with fire intensity patterns in northeastern and central Europe reported by Marlon et al. (2013), which during this time they hypothesise to be driven primarily by human activity. Hence, alongside the use of the climate-driven baseline in our study, high charcoal index, KK10 index and long history of archaeological evidence of human presence across the Mediterranean region support our findings that suggest high human pressure on vegetation “naturalness” of the region and call for a more extensive analysis of HPI against charcoal records. Thus, our findings do not support the hypothesis of a relatively natural land-cover in the Mid-Holocene in Europe, and suggest high levels of anthropogenic modifications to vegetation composition due to cumulative effect of changes introduced by early agricultural and non-agricultural activities.

The HPI values indicate that at TW1 (present –100 BP) nearly 87% of the studied land-cover differed from the potential natural state, which accounts for changes due to agricultural activity as well as impact of non-agricultural activities, accumulated throughout the long history of

human-environment interaction. These values are comparable with previously published estimates, indicating that from 75 to 95% of the global area is somewhat transformed by human societies (Ellis et al., 2010, 2021; Williams et al., 2015). It is, however, challenging to estimate the full extent of anthropogenic impact on land-cover from the existing literature, as lands that are described as “natural” often exhibit long histories of use, including protected areas, managed forest and cultural landscapes (Ellis et al., 2021). Using a quantitative approach, our results validated high levels of cumulative anthropogenic change of vegetation cover at 6000 BP (nearly 72%) and in the modern period (nearly 87%) and emphasized that while agriculture was an important driver of land-cover change in the Holocene, other human practices also significantly contributed to divergence of land-cover from its natural state. Similar conclusions were reported by Strona et al. (2016), who compared forest structure data with PNV simulations, and indicated that at present day European forests are far from a natural condition, showing only moderate signals of the ecological spatial structure typical of undisturbed vegetation (mostly at higher latitudes). It should be noted that while HPI values reflect time-cumulative anthropogenic impact on landscapes, they do not represent exclusively unstable or disturbed ecosystems. If, after an anthropogenic disturbance, an area recovered into a stable and mature ecosystem which is different to the existing pre-disturbance ecosystem, it is still considered to have been altered by human activity through our analysis. Hence, our findings are not directly comparable with a concept of disturbed ecosystems used in ecology, since this study quantifies magnitude by which humans shifted vegetation off its natural climate-driven course regardless of the end-state of the resulting ecosystem. Our findings, however, contribute to the debate on the start of Anthropocene (Lewis and Maslin, 2015; Ruddiman et al., 2016; Ruddiman, 2013, 2018; Smith and Zeder, 2013; Waters et al., 2016; Zalasiewicz et al., 2021), highlighting the importance of acknowledging the long history of anthropogenic land-cover modifications.

## 5. Conclusions

In this study we examined the relationship between simulated potential vegetation (PNV) and pollen-based regional estimates of vegetation abundance (REVEALS) to quantify human pressure on land-cover over the second half of the Holocene (6200 CE). With this method we observed a northward increase of anthropogenic pressure in time, expressed in a form of a human pressure index (HPI) in the largest part of continental Europe (41–54°N) throughout the second half of the Holocene. The time and location of this increase coincide in trajectory and evolution with well-known anthropogenic land-cover change (ALCC) scenarios, KK10 and HYDE 3.2, as well as with findings of the ArchaeoGLOBE initiative. Similar to KK10 and Archaeoglobe, in the Mid-Holocene HPI values suggest anthropogenic land-cover modifications across Mediterranean Europe, and partial modifications in central and northern Europe. From there, HPI extends towards the north, with increasing intensity around 1200–1700 BP, following patterns similar to the ALCC scenarios. Our study found that almost 60% of grid cells exhibited a significant increase in HPI values during the modern time (TW1), compared to 5700–6200 BP (TW14). These findings align with estimates of ALCC: nearly 56% of the study area’s land-cover was transformed by human activities during the modern era (TW1) based on KK10 estimates, while HYDE 3.2 estimates suggest that agriculture impacted nearly 45% of the land-cover, with grazing accounting for 18% and cropland accounting for 27%. However, our inferred human impact on vegetation (as indicated by HPI values) was greater than suggested by the KK10 deforestation index, and HYDE 3.2 cropland and grazing estimates. We observed high initial values of HPI at 5700–6200 BP, indicating up to 70% of the vegetation composition was affected by humans, as well as the absence of correlation between presence of agricultural taxa in REVEALS. These findings suggest that our approach demonstrates human impact on land-cover in a broader aspect than agriculture.

Significant correlation of HPI with HYDE 3.2 population density ( $r = 0.75$ ,  $p$ -value  $< 0.005$ ) indicates that the HPI is strongly associated with human activity. Our findings suggest that up to 70% of vegetation composition in Europe may have been affected by both early agricultural and pre-agricultural human practices prior to the Mid-Holocene. In the context of the debate about the chronology of the Anthropocene, this study suggests that anthropogenic land-cover change transcends the boundaries of agriculture. It highlights the significance of cumulative effect of pre-agricultural practices on the state of land-cover in the Mid-Holocene, and calls for a more comprehensive exploration of the complex interactions between humans and the environment during that era.

## Credit author statement

**Anhelina Zapolska:** Conceptualization, Methodology, Software, Formal analysis, Investigation, Writing - Original Draft. **Maria Antonia Serge:** Investigation, Resources, Data Curation, Writing - Review & Editing. **Florence Mazier:** Conceptualization, Investigation, Resources, Data Curation, Writing - Review & Editing. **Aurélien Quiquet:** Software, Methodology, Writing - Review & Editing. **Hans Renssen:** Methodology, Software, Writing - Review & Editing, Supervision. **Mathieu Vrac:** Software, Methodology, Writing - Review & Editing. **Ralph Fyfe:** Investigation, Resources, Writing - Review & Editing. **Didier M. Roche:** Conceptualization, Methodology, Software, Investigation, Writing - Original Draft, Supervision, Project administration.

## Funding

The research is financed through the European Union’s Horizon 2020 research and innovation programme within the TERRANOVA project, No 813904, and supported by the Vrije Universiteit Amsterdam. The paper reflects the views only of the authors, and the European Union cannot be held responsible for any use which may be made of the information contained therein.

The study is also a contribution to the Past Global Change (PAGES) project and its working group LandCover6k that in turn received support from the Swiss National Science Foundation, the Swiss Academy of Sciences, the U.S. National Science Foundation, and the Chinese Academy of Sciences.

## Declaration of competing interest

The authors declare that they have no known competing financial interests or personal relationships that could have appeared to influence the work reported in this paper.

## Data availability

The data produced within this study are available in the supplementary materials to the article.

## Acknowledgements

The authors would like to thank Louis M. François for providing the CARAIB global dynamic vegetation model and his help in running it. We would also like to express our sincere appreciation to Emily Vella, Kailin Hatlestad, Alexandre Martinez and Anastasia Nikulina for their invaluable contributions and expertise during the review process, and to two anonymous reviewers for valuable comments that improved the quality of the paper.

## Appendix A. Supplementary data

Supplementary data to this article can be found online at <https://doi.org/10.1016/j.quascirev.2023.108227>.

## References

- Archibald, S., Staver, A.C.C., Levin, S.A., 2012. Evolution of human-driven fire regimes in Africa. *Proc. Natl. Acad. Sci. U. S. A* 109, 847–852. <https://doi.org/10.1073/pnas.1118648109>.
- Arthur, F., Roche, D.M., Fyfe, R., Quiquet, A., Renssen, H., 2022. Simulations of the Holocene climate in Europe using dynamical downscaling within the iLOVECLIM model (version 1.1). *Clim. Past*. <https://doi.org/10.5194/cp-2022-21>.
- Bartlein, P.J., Harrison, S.P., Brewer, S., Connor, S., Davis, B.A.S., Gajewski, K., Guiot, J., Harrison-Prentice, T.I., Henderson, A., Peyron, O., Prentice, I.C., Scholze, M., Seppä, H., Shuman, B., Sugita, S., Thompson, R.S., Vial, A.E., Williams, J., Wu, H., 2011. Pollen-based continental climate reconstructions at 6 and 21 ka: a global synthesis. *Clim. Dynam.* 37, 775–802. <https://doi.org/10.1007/s00382-010-0904-1>.
- Bauer, A.M., Edgeworth, M., Edwards, L.E., Ellis, E.C., Gibbard, P., Merritts, D.J., 2021. Anthropocene: event or epoch? *Nature* 597, 332. <https://doi.org/10.1038/D41586-021-02448-Z>.
- Behre, K.-E., 1981. The interpretation of anthropogenic indicators in pollen diagrams. *Cent. Natl. la Rech. Sci.* 225, 245.
- Berger, A.L., 1978. Long-term variations of daily insolation and Quaternary climatic changes. *J. Atmos. Sci.* 35, 2361–2367. [https://doi.org/10.1175/1520-0469\(1978\)035<2362:ltvodi>2.0.co;2](https://doi.org/10.1175/1520-0469(1978)035<2362:ltvodi>2.0.co;2).
- Bos, J.A.A.A., Urz, R., 2003. Late Glacial and early Holocene environment in the middle Lahn river valley (Hessen, central-west Germany) and the local impact of early Mesolithic people—pollen and macrofossil evidence. *Veg. Hist. Archaeobotany* 12, 19–36. <https://doi.org/10.1007/s00334-003-0006-7>.
- Bouttes, N., Lhardy, F., Quiquet, A., Paillard, D., Goussé, H., Roche, D.M., 2023. Deglacial climate changes as forced by ice sheet reconstructions. *EGU Sph. Prepr.* <https://doi.org/10.5194/egusphere-2022-993>.
- Braje, T.J., Erlandson, J.M., 2013a. Human acceleration of animal and plant extinctions: a Late Pleistocene, Holocene, and Anthropocene continuum. *Anthropocene* 4, 14–23. <https://doi.org/10.1016/J.ANCENE.2013.08.003>.
- Braje, T.J., Erlandson, J.M., 2013b. Looking forward, looking back: humans, anthropogenic change, and the Anthropocene. *Anthropocene* 4, 116–121. <https://doi.org/10.1016/j.ancene.2014.05.002>.
- Brovkin, V., Ganopolski, A., Svirezhev, Y., 1997. A continuous climate-vegetation classification for use in climate-biosphere studies. *Ecol. Model.* 101, 251–261. [https://doi.org/10.1016/S0304-3800\(97\)00049-5](https://doi.org/10.1016/S0304-3800(97)00049-5).
- Carracedo, V., Cunill, R., García-Codron, J.C., Pélachs, A., Pérez-Obiol, R., Soriano, J.M., 2018. History of fires and vegetation since the neolithic in the cantabrian mountains (Spain). *Land Degrad. Dev.* 29, 2060–2072. <https://doi.org/10.1002/LDR.2891>.
- Certini, G., Scalenghe, R., 2011. Anthropogenic soils are the golden spikes for the Anthropocene. *Holocene* 21, 1269–1274. [https://doi.org/10.1177/0959683611408454/ASSET/IMAGES/LARGE/10.1177\\_0959683611408454-FIG2.JPG](https://doi.org/10.1177/0959683611408454/ASSET/IMAGES/LARGE/10.1177_0959683611408454-FIG2.JPG).
- Connor, S.E., Vannière, B., Colombaroli, D., Anderson, R.S., Carrión, J.S., Ejarque, A., Gil Romera, G., González-Sampériz, P., Hoefler, D., Morales-Molino, C., Revelles, J., Schneider, H., van der Knaap, W.O., van Leeuwen, J.F.N., Woodbridge, J., 2019. Humans take control of fire-driven diversity changes in Mediterranean Iberia's vegetation during the mid-late Holocene. *Holocene* 29, 886–901. <https://doi.org/10.1177/0959683619826652>.
- Crutzen, P.J., 2002. The “anthropocene.” *J. Phys. IV*, 12. [https://doi.org/10.1051/JP4:20020447\\_1-5](https://doi.org/10.1051/JP4:20020447_1-5).
- Cruz-Silva, E., Harrison, S.P., Marinova, E., Prentice, I.C., 2022. A new method based on surface-sample pollen data for reconstructing palaeovegetation patterns. *J. Biogeogr.* 49, 1381–1396. <https://doi.org/10.1111/JBL14448>.
- Dallmeyer, A., Claussen, M., Brovkin, V., 2019. Harmonising plant functional type distributions for evaluating Earth system models. *Clim. Past* 15, 335–366. <https://doi.org/10.5194/cp-15-335-2019>.
- Dallmeyer, A., Poska, A., Marquer, L., Seim, A., Gaillard-Lemdhall, M.-J., 2023. the challenge of comparing pollen-based quantitative vegetation reconstructions with outputs from vegetation models – a European perspective. *Clim. Past Discuss* 1–50. <https://doi.org/10.5194/CP-2023-16>.
- Deza-Araujo, M., Morales-Molino, C., Tinner, W., Henne, P.D., Heitz, C., Pezzatti, G.B., Hafner, A., Conedera, M., 2020. A critical assessment of human-impact indices based on anthropogenic pollen indicators. *Quat. Sci. Rev.* 236, 106291. <https://doi.org/10.1016/J.QUASCIREV.2020.106291>.
- Deza-Araujo, M., Morales-Molino, C., Conedera, M., Henne, P.D., Krebs, P., Hinz, M., Heitz, C., Hafner, A., Tinner, W., 2022. A new indicator approach to reconstruct agricultural land use in Europe from sedimentary pollen assemblages. *Palaeogeogr. Palaeoclimatol. Palaeoecol.* 599, 111051. <https://doi.org/10.1016/J.PALAEO.2022.111051>.
- Dietze, E., Theuerkauf, M., Bloom, K., Brauer, A., Dörfler, W., Feeser, I., Feurdean, A., Gedminiene, L., Giesecke, T., Jahns, S., Karpińska-Kotaczek, M., Kotaczek, P., Lamentowicz, M., Latalowa, M., Marcisz, K., Obremaska, M., Pędziszewska, A., Poska, A., Rehfeld, K., Stancikaite, M., Stivrins, N., Święta-Musznicka, J., Szal, M., Vassiljev, J., Veski, S., Wacnik, A., Weisbrodt, D., Wiethold, J., Vannière, B., Stowiński, M., Dörfler, W., Feeser, I., Feurdean, A., Gedminiene, L., Giesecke, T., Jahns, S., Karpińska-Kotaczek, M., Kotaczek, P., Lamentowicz, M., Latalowa, M., Marcisz, K., Obremaska, M., Pędziszewska, A., Poska, A., Rehfeld, K., Stancikaite, M., Stivrins, N., Święta-Musznicka, J., Szal, M., Vassiljev, J., Veski, S., Wacnik, A., Weisbrodt, D., Wiethold, J., Vannière, B., Stowiński, M., 2018. Holocene fire activity during low-natural flammability periods reveals scale-dependent cultural human-fire relationships in Europe. *Quat. Sci. Rev.* 201, 44–56. <https://doi.org/10.1016/j.quascirev.2018.10.005>.
- Doughty, C.E., 2013. Preindustrial human impacts on global and regional environment. *Annu. Rev. Environ. Resour.* 38, 503–527. <https://doi.org/10.1146/annurev-environ-032012-095147>.
- Dury, M., Hamburgers, A., Warnant, P., Henrot, A., Favre, E., Ouberdous, M., François, L., 2011. Responses of European forest ecosystems to 21st century climate: assessing changes in interannual variability and fire intensity. *IForest* 4, 82–99. <https://doi.org/10.3832/ifer0572-004>.
- Edgeworth, M., Richter, D.D.B., Waters, C., Haff, P., Neal, C., Price, S.J., 2015. Diachronous beginnings of the anthropocene: the lower bounding surface of anthropogenic deposits. *Anthropol. Rev.* 2, 33–58. [https://doi.org/10.1177/2053019614565394/ASSET/IMAGES/LARGE/10.1177\\_2053019614565394-FIG2.JPG](https://doi.org/10.1177/2053019614565394/ASSET/IMAGES/LARGE/10.1177_2053019614565394-FIG2.JPG).
- Edwards, L.E., Edgeworth, M., Ellis, E.C., Leonard Gibbard, P., 2022. The Anthropocene serves science better as an event, rather than an epoch the analysis of the topographic signature of anthropogenic geomorphic processes View project Continental Shelves, Drowned Landscapes, North Sea Palaeogeography View project. *Artic. J. Quat. Sci.* <https://doi.org/10.1002/jqs.3475>.
- Ellis, E.C., Goldewijk, K.K., Siebert, S., Lightman, D., Ramankutty, N., 2010. Anthropogenic transformation of the biomes, 1700 to 2000. *Global Ecol. Biogeogr.* 19, 589–606.
- Ellis, E.C., Kaplan, J.O., Fuller, D.Q., Vavrus, S., Goldewijk, K.K., Verburg, P.H., 2013. Used planet: a global history. <https://doi.org/10.1073/pnas.1217241110>, 14 May.
- Ellis, E.C., Gauthier, N., Goldewijk, K.K., Bird, R.B., Boivin, N., Díaz, S., Fuller, D.Q., Gill, J.L., Kaplan, J.O., Kingston, N., Locke, H., McMichael, C.N.H.H., Ranco, D., Rick, T.C., Rebecca Shaw, M., Stephens, L., Svenning, J.C., Watson, J.E.M.M., 2021. People have shaped most of terrestrial nature for at least 12,000 years. *Proc. Natl. Acad. Sci. U. S. A* 118, 1–8. <https://doi.org/10.1073/pnas.2023483118>.
- Erlandson, J.M., Braje, T.J., 2013. Archeology and the anthropocene. *Anthropocene* 4, 1–7. <https://doi.org/10.1016/j.ancene.2014.05.003>.
- FAO, 2022. FAO Publications Catalogue 2022. FAO, Rome, Italy. <https://doi.org/10.4060/cc2323en>.
- Farris, E., Filibeck, G., Marignani, M., Rosati, L., 2010. The power of potential natural vegetation (and of spatial-temporal scale): a response to Carrión & Fernández (2009). *J. Biogeogr.* 37, 2211–2213. <https://doi.org/10.1111/J.1365-2699.2010.02323.X>.
- Finsinger, W., Tinner, W., Van Der Knaap, W.O., Ammann, B., 2006. The expansion of hazel (*Corylus avellana* L.) in the southern Alps: a key for understanding its early Holocene history in Europe? *Quat. Sci. Rev.* 25, 612–631. <https://doi.org/10.1016/J.QUASCIREV.2005.05.006>.
- Foley, S.F., Gronenborn, D., Andrae, M.O., Kadereit, J.W., Esper, J., Scholz, D., Pöschl, U., Jacob, D.E., Schöne, B.R., Schreg, R., Vött, A., Jordan, D., Lelieveld, J., Weller, C.G., Alt, K.W., Gaudzinski-Windheuser, S., Bruhn, K.C., Tost, H., Sirocko, F., Crutzen, P.J., 2013. The Palaeoanthropocene – the beginnings of anthropogenic environmental change. *Anthropocene* 3, 83–88. <https://doi.org/10.1016/J.ANCENE.2013.11.002>.
- François, L.M., Delire, C., Warnant, P., Munhoven, G., 1998. Modelling the glacial-interglacial changes in the continental biosphere. *Global Planet. Change* 16, 37–52. [https://doi.org/10.1016/S0921-8181\(98\)00005-8](https://doi.org/10.1016/S0921-8181(98)00005-8).
- François, L.M., Utescher, T., Favre, E., Henrot, A.J., Warnant, P., Micheels, A., Erdei, B., Suc, J.P., Cheddadi, R., Mosbrugger, V., 2011. Modelling Late Miocene vegetation in Europe: results of the CARAIB model and comparison with palaeovegetation data. *Palaeogeogr. Palaeoclimatol. Palaeoecol.* 304, 359–378. <https://doi.org/10.1016/J.PALAEO.2011.01.012>.
- Fyfe, R.M., Twiddle, C., Sugita, S., Gaillard, M.-J., Barratt, P., Caseldine, C.J., Dodson, J., Edwards, K.J., Farrell, M., Froyd, C., Grant, M.J., Huckerby, E., Innes, J.B., Shaw, H., Waller, M., 2013. The Holocene vegetation cover of Britain and Ireland: overcoming problems of scale and discerning patterns of openness. *Quat. Sci. Rev.* 73, 132–148. <https://doi.org/10.1016/j.quascirev.2013.05.014>.
- Fyfe, R.M., Woodbridge, J., Roberts, N., 2015. From forest to farmland: pollen-inferred land change across Europe using the pseudobionization approach. *Global Change Biol.* 21, 1197–1212. <https://doi.org/10.1111/GCB.12776>.
- Fyfe, R.M., Woodbridge, J., Palmisano, A., Bevan, A., Shennan, S., Burjachs, F., Legarra Herrero, B., García Puchol, O., Carrión, J.S., Revelles, J., Roberts, C.N., 2019. Prehistoric palaeodemographics and regional land cover change in eastern Iberia. *Holocene* 29, 799–815. [https://doi.org/10.1177/0959683619826643/ASSET/IMAGES/LARGE/10.1177\\_0959683619826643-FIG6.JPG](https://doi.org/10.1177/0959683619826643/ASSET/IMAGES/LARGE/10.1177_0959683619826643-FIG6.JPG).
- Gaillard, M.-J., 2007. POLLEN methods and studies | archaeological applications. *Encycl. Quat. Sci.* 2570–2595. <https://doi.org/10.1016/B0-44-452747-8/00214-3>.
- Gaillard, M.-J., 2013. Pollen methods and studies. *Archaeological applications*. In: Elias, S., Mock, C.J. (Eds.), *Encyclopedia of Quaternary Science*, second ed. Elsevier, Amsterdam, pp. 880–904. <https://doi.org/10.1016/B978-0-444-53643-3.00182-5>.
- Gaillard, M.-J., Sugita, S., Mazier, F., Trondman, A.K., Broström, A., Hickler, T., Kaplan, J.O., Kjellström, E., Kokfelt, U., Kuneš, P., Lemmen, C., Miller, P., Olofsson, J., Poska, A., Rundgren, M., Smith, B., Strandberg, G., Fyfe, R., Nielsen, A. B., Alenius, T., Balakauskas, L., Barnekow, L., Birks, H.J.B., Bjune, A., Björkman, L., Giesecke, T., Hjelke, K., Kalnina, L., Kangur, M., Van Der Knaap, W.O., Koff, T., Lageras, P., Latalowa, M., Leydet, M., Lechterbeck, J., Lindbladh, M., Odgaard, B., Peglar, S., Segerström, U., Von Stedingk, H., Seppä, H., 2010. Holocene land-cover reconstructions for studies on land cover-climate feedbacks. *Clim. Past* 6, 483–499. <https://doi.org/10.5194/cp-6-483-2010>.
- Gibbard, P., Walker, M., Bauer, A., Edgeworth, M., Edwards, L., Ellis, E., Finney, S., Gill, J.L., Maslin, M., Merritts, D., Ruddiman, W., 2022. The anthropocene as an event, not an epoch. *J. Quat. Sci.* 37, 395–399. <https://doi.org/10.1002/JQS.3416>.
- Github, E., Fyfe, R., Gaillard, M.-J., Trondman, A.K., Mazier, F., Nielsen, A.B., Poska, A., Sugita, S., Woodbridge, J., Azuara, J., Feurdean, A., Grindean, R., Lebreton, V., Marquer, L., Nebout-Combouret, N., Stancikaite, M., Tanțău, I.,



- Tonkov, S., Shumilovskikh, L., Åkesson, C., Balakauskas, L., Batalova, V., Birks, H.J. B., Bjune, A.E., Borisova, O., Bozilova, E., Burjachs, F., Cheddadi, R., Christiansen, J., David, R., De Klerk, P., Di Rita, F., Dörfler, W., Doyen, E., Eastwood, W., Etienne, D., Feeser, I., Filipova-Marinova, M., Fischer, E., Galop, D., Carrion, J.G.S., Gauthier, E., Giesecke, T., Herking, C., Herzschuh, U., Jouffroy-Bapicot, I., Kasianova, A., Kouli, K., Kuneš, P., Lagerås, P., Latalowa, M., Lechterbeck, J., Leroyer, C., Leydet, M., Lisystina, O., Lukanina, E., Magyari, E., Marguerie, D., Lippi, M.M., Mensing, S., Mercuri, A.M., Miebach, A., Milburn, P., Miras, Y., Del Molino, C.M., Mrotzek, A., Nosova, M., Odgaard, B.V., Overballe-Petersen, M., Panajiotidis, S., Pavlov, D., Persson, T., Pinke, Z., Ruffaldi, P., Sapelko, T., Schmidt, M., Schult, M., Stivrins, N., Tarasov, P.E., Theuerkauf, M., Veski, S., Wick, L., Wiethold, J., Woldring, H., Zernitskaya, V., 2022. European pollen-based REVEALS land-cover reconstructions for the Holocene: methodology, mapping and potentials. *Earth Syst. Sci. Data* 14, 1581–1619. <https://doi.org/10.5194/ESSD-14-1581-2022>.
- Goldewijk, K.K., Beusen, A., Janssen, P., 2010. Long-term dynamic modeling of global population and built-up area in a spatially explicit way: HYDE 3.1. *Holocene* 20, 565–573.
- Goldewijk, K.K., Beusen, A., Van Drecht, G., De Vos, M., 2011. The HYDE 3.1 spatially explicit database of human-induced global land-use change over the past 12,000 years. *Global Ecol. Biogeogr.* 20, 73–86. <https://doi.org/10.1111/j.1466-8238.2010.00587.x>.
- Goldewijk, K.K., Doelman, J., Stehfest, E., 2017a. Anthropogenic land use estimates for the Holocene - HYDE 3.2. *Earth Syst. Sci. Data* 9, 927–953. <https://doi.org/10.5194/essd-9-927-2017>.
- Goldewijk, K.K., Dekker, S.C., van Zanden, J.L., 2017b. Per-capita estimations of long-term historical land use and the consequences for global change research. *J. Land Use Sci.* 12, 313–337. <https://doi.org/10.1080/1747423X.2017.1354938>.
- Goosse, H., Fichefet, T., 1999. Importance of ice-ocean interactions for the global ocean circulation: a model study. *J. Geophys. Res. Ocean.* 104, 23337–23355. <https://doi.org/10.1029/1999jc900215>.
- Goosse, H., Brovkin, V., Fichefet, T., Haarsma, R., Huybrechts, P., Jongma, J., Mouchet, A., Selten, F., Barriat, P.Y., Campin, J.M., Deleersnijder, E., Driesschaert, E., Goelzer, H., Janssens, I., Loutre, M.F., Morales Maqueda, M.A., Opsteegh, P., Mathieu, P.P., Munhoven, G., Pettersson, E.J., Renssen, H., Roche, D. M., Schaeffer, M., Tartinville, B., Timmermann, A., Weber, S.L., 2010. Description of the Earth system model of intermediate complexity LOVECLIM version 1.2. *Geosci. Model Dev* 3, 603–633. <https://doi.org/10.5194/GMD-3-603-2010>.
- Gronenborn, D., Horejs, B., 2021. Expansion of Farming in Western Eurasia, 9600 - 4000 Cal BC (Update Vers. 2021.2). <https://doi.org/10.5281/ZENODO.5903165>. Zenodo.
- Harrison, S.P., Gaillard, M.-J., Stocker, B.D., Vander Linden, M., Klein Goldewijk, K., Boles, O., Braconnot, P., Dawson, A., Fluet-Chouinard, E., Kaplan, J.O., Kastner, T., Pausata, F.S.R., Robinson, E., Whitehouse, N.J., Madella, M., Morrison, K.D., Goldewijk, K.K., Boles, O., Braconnot, P., Dawson, A., Fluet-Chouinard, E., Kaplan, J. O., Kastner, T., Pausata, F.S.R., Robinson, E., Whitehouse, N.J., Madella, M., Morrison, K.D., 2020. Development and testing scenarios for implementing land use and land cover changes during the Holocene in Earth system model experiments. *Geosci. Model Dev. (GMD)* 13, 805–824. <https://doi.org/10.5194/GMD-13-805-2020>.
- Head, M.J., Steffen, W., Fagerlind, D., Waters, C.N., Poirier, C., Syvitski, J., Zalasiewicz, J.A., Barnosky, A.D., Cearreta, A., Jeandel, C., Leinfelder, R., McNeill, J. R., Rose, N.L., Summerhayes, C., Wagreich, M., Zinke, J., 2022a. The Great Acceleration is real and provides a quantitative basis for the proposed Anthropocene Series/Epoch. *Episodes J. Int. Geosci.* 45, 359–376. <https://doi.org/10.18814/EPJUGS/2021/021031>.
- Head, M.J., Zalasiewicz, J.A., Waters, C.N., Turner, S.D., Williams, M., Barnosky, A.D., Steffen, W., Wagreich, M., Haff, P.K., Syvitski, J., Leinfelder, R., McCarthy, F.M.G., Rose, N.L., Wing, S.L., An, Z., Cearreta, A., Cundy, A.B., Fairchild, I.J., Han, Y., Ivar Do Sul, J.A., Jeandel, C., McNeill, J.R., Summerhayes, C.P., 2022b. The proposed Anthropocene Epoch/Series is underpinned by an extensive array of mid-20th century stratigraphic event signals. *J. Quat. Sci.* 37, 1181–1187. <https://doi.org/10.1002/JQS.3467>.
- Hengl, T., Walsh, M.G., Sanderman, J., Wheeler, I., Harrison, S.P., Prentice, I.C., 2018. Global mapping of potential natural vegetation: an assessment of machine learning algorithms for estimating land potential. *PeerJ*, 2018. <https://doi.org/10.7717/peerj.5457>.
- Henrot, A.J., Utescher, T., Erdei, B., Dury, M., Hamon, N., Ramstein, G., Krapp, M., Herold, N., Goldner, A., Favre, E., Munhoven, G., François, L., 2017. Middle Miocene climate and vegetation models and their validation with proxy data. *Palaeogeogr. Palaeoclimatol. Palaeoecol.* 467, 95–119. <https://doi.org/10.1016/j.palaeo.2016.05.026>.
- Hiscock, P., Attenbrow, V., 2016. Dates and demography? The need for caution in using radiometric dates as a robust proxy for prehistoric population change. *Archaeol. Ocean.* 51, 218–219. <https://doi.org/10.1002/ARCO.5096>.
- Jackson, S.T., 2013. Natural, potential and actual vegetation in North America. *J. Veg. Sci.* 24, 772–776. <https://doi.org/10.1111/JVS.12004>.
- Kalis, A.J., Merkt, J., Wunderlich, J., 2003. Environmental changes during the Holocene climatic optimum in central Europe - human impact and natural causes. *Quat. Sci. Rev.* 22, 33–79. [https://doi.org/10.1016/S0277-3791\(02\)00181-6](https://doi.org/10.1016/S0277-3791(02)00181-6).
- Kaplan, J.O., Krumhardt, K.M., 2011. The KK10 Anthropogenic Land Cover Change Scenario for the Preindustrial Holocene. *PANGAEA*. <https://doi.org/10.1594/PANGAEA.871369>.
- Kaplan, J.O., Krumhardt, K.M., Zimmermann, N., 2009. The prehistoric and preindustrial deforestation of Europe. *Quat. Sci. Rev.* 28, 3016–3034. <https://doi.org/10.1016/j.quascirev.2009.09.028>.
- Kaplan, J.O., Krumhardt, K.M., Ellis, E.C., Ruddiman, W.F., Lemmen, C., Goldewijk, K.K., 2011. Holocene carbon emissions as a result of anthropogenic land cover change. *Holocene* 21, 775–791. <https://doi.org/10.1177/0959683610386983>.
- Kaplan, J.O., Krumhardt, K.M., Gaillard, M.-J., Sugita, S., Trondman, A.-K.K., Fyfe, R., Marquer, L., Mazier, F., Nielsen, A.B., 2017. Constraining the deforestation history of Europe: evaluation of historical land use scenarios with pollen-based land cover reconstructions. *Land* 6, 91. <https://doi.org/10.3390/land6040091>.
- Koch, P.L., Barnosky, A.D., 2006. Late Quaternary Extinctions: State of the Debate, vol. 37, pp. 215–250. <https://doi.org/10.1146/annurev.ecolsys.34.011802.132415>.
- Kuosmanen, N., Marquer, L., Tallavaara, M., Molinari, C., Zhang, Y., Alenius, T., Edinborough, K., Pesonen, P., Reitalu, T., Renssen, H., Trondman, A.K., Seppä, H., 2018. The role of climate, forest fires and human population size in Holocene vegetation dynamics in Fennoscandia. *J. Veg. Sci.* 29, 382–392.
- Lange, S., 2016. Earth2Observe, WFDEI and ERA-Interim Data Merged and Bias-Corrected for ISIMIP (EWEMBI). *GFZ Data Serv.*
- Laurent, J.M., François, L.M., Bar-Hen, A., Bel, L., Cheddadi, R., 2008. European bioclimatic affinity groups: data-model comparisons. *Global Planet. Change* 61, 28–40. <https://doi.org/10.1016/j.gloplacha.2007.08.017>.
- Lechterbeck, J., Edinborough, K., Kerig, T., Fyfe, R., Roberts, N., Shennan, S., 2014. Is Neolithic land use correlated with demography? An evaluation of pollen-derived land cover and radiocarbon-inferred demographic change from Central Europe. *Holocene* 24, 1297–1307. [https://doi.org/10.1177/0959683614540952/ASSET/IMAGES/LARGE/10.1177\\_0959683614540952-FIG4.JPEG](https://doi.org/10.1177/0959683614540952/ASSET/IMAGES/LARGE/10.1177_0959683614540952-FIG4.JPEG).
- Lemmen, C., 2009. World distribution of land cover changes during Pre-and Protohistoric Times and estimation of induced carbon releases. *Geoarchaeology human-environment Connect* 15, 303–312. <https://doi.org/10.4000/geomorphologie.7756>.
- Levassieur, G., Vrac, M., Roche, D.M., Paillard, D., 2012. Statistical modelling of a new global potential vegetation distribution. *Environ. Res. Lett.* 7, 44019–44030. <https://doi.org/10.1088/1748-9326/7/4/044019>.
- Levassieur, G., Vrac, M., Roche, D.M., Paillard, D., Guiot, J., 2013. An objective methodology for potential vegetation reconstruction constrained by climate. *Global Planet. Change* 104, 7–22. <https://doi.org/10.1016/J.GLOPLACHA.2013.01.008>.
- Lewis, S.L., Maslin, M.A., 2015. Defining the anthropocene. *Nat.* 2015 5197542 519, 171–180. <https://doi.org/10.1038/nature14258>.
- Lightfoot, K.G., Cuthrell, R.Q., 2015. Anthropogenic burning and the Anthropocene in late-Holocene California. *Holocene* 25, 1581–1587. <https://doi.org/10.1177/0959683615588376>.
- Livi-Bacci, M., 2007. *A concise history of world population*, 4th edn. Blackwell Publishing, Oxford, UK.
- Loidi, J., del Arco, M., Pérez de Paz, P.L., Asensi, A., Díez Garretas, B., Costa, M., Díaz González, T., Fernández-González, F., Izco, J., Penas, A., Rivas-Martínez, S., Sánchez-Mata, D., 2010. Understanding properly the 'potential natural vegetation' concept. *J. Biogeogr.* 37, 2209–2211. <https://doi.org/10.1111/J.1365-2699.2010.02302.X>.
- Maddison, A., 2001. *The World Economy*. OECD, Paris, France. <https://doi.org/10.1787/9789264189980-EN>.
- Mann, D.H., Groves, P., Gaglioti, B.V., Shapiro, B.A., 2019. Climate-driven ecological stability as a globally shared cause of Late Quaternary megafaunal extinctions: the Plaids and Stripes Hypothesis. *Biol. Rev.* 94, 328–352. <https://doi.org/10.1111/BRV.12456>.
- Marlon, J.R., Bartlein, P.J., Danianu, A.L., Harrison, S.P., Maezumi, S.Y., Power, M.J., Tinner, W., Vannié, B., 2013. Global biomass burning: a synthesis and review of Holocene paleofire records and their controls. *Quat. Sci. Rev.* 65, 5–25. <https://doi.org/10.1016/J.QUASCIREV.2012.11.029>.
- Marquer, L., Gaillard, M.-J., Sugita, S., Trondman, A.K., Mazier, F., Nielsen, A.B., Fyfe, R. M., Odgaard, B.V., Alenius, T., Birks, H.J.B., Bjune, A.E., Christiansen, J., Dodson, J., Edwards, K.J., Giesecke, T., Herzschuh, U., Kangur, M., Lorenz, S., Poska, A., Schult, M., Seppä, H., 2014. Holocene changes in vegetation composition in northern Europe: why quantitative pollen-based vegetation reconstructions matter. *Quat. Sci. Rev.* 90, 199–216. <https://doi.org/10.1016/J.QUASCIREV.2014.02.013>.
- Marquer, L., Gaillard, M.-J., Sugita, S., Poska, A., Trondman, A.K., Mazier, F., Nielsen, A. B., Fyfe, R.M., Jönsson, A.M., Smith, B., Kaplan, J.O., Alenius, T., Birks, H.J.B., Bjune, A.E., Christiansen, J., Dodson, J., Edwards, K.J., Giesecke, T., Herzschuh, U., Kangur, M., Koff, T., Latalowa, M., Lechterbeck, J., Olofsson, J., Seppä, H., 2017. Quantifying the effects of land use and climate on Holocene vegetation in Europe. *Quat. Sci. Rev.* 171, 20–37.
- Mazier, F., Gaillard, M.-J., Kuneš, P., Sugita, S., Trondman, A.K., Broström, A., 2012. Testing the effect of site selection and parameter setting on REVEALS-model estimates of plant abundance using the Czech Quaternary Palynological Database. *Rev. Palaeobot. Palynol.* 187, 38–49. <https://doi.org/10.1016/j.revpalbo.2012.07.017>.
- McEvedy, C., Jones, R., 1978. *Atlas of World Population History*, vols. 1–368. Penguin Books Ltd, Northwestern University, Hammondsworth, UK.
- McWethy, D.B., Whitlock, C., Wilmshurst, J.M., McGlone, M.S., Fromont, M., Li, X., Dieffenbacher-Krall, A., Hobbs, W.O., Fritz, S.C., Cook, E.R., 2010. Rapid landscape transformation in South Island, New Zealand, following initial Polynesian settlement. *Proc. Natl. Acad. Sci. U. S. A.* 107, 21343–21348. [https://doi.org/10.1073/PNAS.1011801107/SUPPL\\_FILE/PNAS.1011801107\\_SI.PDF](https://doi.org/10.1073/PNAS.1011801107/SUPPL_FILE/PNAS.1011801107_SI.PDF).
- Mercuri, A.M., Bandini Mazzanti, M., Florenzano, A., Montecchi, M.C., Rattighieri, E., 2013. Olea, Juglans and Castanea: the OJG group as pollen evidence of the development of human-induced environments in the Italian peninsula. *Quat. Int.* 303, 24–42. <https://doi.org/10.1016/J.QUAINT.2013.01.005>.
- Morrison, K.D., Hammer, E., Boles, O., Madella, M., Whitehouse, N., Gaillard, M.J., Bates, J., Linden, M., Vander Merlo, S., Yao, A., Popova, L., Hill, A.C., Antolin, F., Bauer, A., Biagetti, S., Bishop, R.R., Buckland, P., Cruz, P., Dreslerová, D.,

- Dusseldorp, G., Ellis, E., Filipovic, D., Foster, T., Hannaford, M.J., Harrison, S.P., Hazarika, M., Herold, H., Hilpert, J., Kaplan, J.O., Kay, A., Goldewijk, K.K., Kolár, J., Kyazike, E., Laabs, J., Lancelotti, C., Lane, P., Lawrence, D., Lewis, K., Lombardo, U., Lucarini, G., Arroyo-Kalin, M., Marchant, B., Mayle, F., McClatchie, M., McLeester, M., Mooney, S., Moskal-Del Hoyo, M., Navarrete, V., Ndiema, E., Neves, E.G., Nowak, M., Out, W.A., Petrie, C., Phelps, L.N., Pinke, Z., Rostain, S., Russell, T., Sluyter, A., Styring, A.K., Tamanaha, E., Thomas, E., Veerasamy, S., Welton, L., Zanon, M., 2021. Mapping past human land use using archaeological data: a new classification for global land use synthesis and data harmonization. *PLoS One* 16, e0246662. <https://doi.org/10.1371/JOURNAL.PONE.0246662>.
- Mottl, O., Flantua, S.G.A., Bhatta, K.P., Felde, V.A., Giesecke, T., Goring, Simon, Grimm, E.C., Haberle, S., Hooghiemstra, H., Ivory, S., Kunes, P., Wolters, S., Seddon, A.W.R., Williams, J.W., 2021. Global acceleration in rates of vegetation change over the past 18,000 years. *Science* 372 (80-), 860–864. [https://doi.org/10.1126/SCIENCE.ABG1685/SUPPL\\_FILE/ABG1685\\_MOTTL\\_SM.PDF](https://doi.org/10.1126/SCIENCE.ABG1685/SUPPL_FILE/ABG1685_MOTTL_SM.PDF).
- Nielsen, A.B., Giesecke, T., Theuerkauf, M., Feeser, I., Behre, K.E., Beug, H.J., Chen, S.H., Christiansen, J., Dörfler, W., Endtmann, E., Jahns, S., de Klerk, P., Kühl, N., Latalova, M., Odgaard, B.V., Rasmussen, P., Stockholm, J.R., Voigt, R., Wiethold, J., Wolters, S., 2012. Quantitative reconstructions of changes in regional openness in north-central Europe reveal new insights into old questions. *Quat. Sci. Rev.* 47, 131–149. <https://doi.org/10.1016/j.quascirev.2012.05.011>.
- Nikulina, A., MacDonald, K., Scherjon, F., A Pearce, E., Davoli, M., Svenning, J.C., Vella, E., Gaillard, M.-J., Zapolska, A., Arthur, F., Martinez, A., Hatlestad, K., Mazier, F., Serge, M.A., Lindholm, K.J., Fyfe, R., Renssen, H., Roche, D.M., Kluijver, S., Roebroeks, W., 2022. Tracking hunter-gatherer impact on vegetation in last interglacial and Holocene Europe: proxies and challenges. *J. Archaeol. Method Theor* 29, 989–1033. <https://doi.org/10.1007/s10816-021-09546-2>.
- O'Dwyer, R., Marquer, L., Trondman, A.K., Jönsson, A.M., 2021. Spatially continuous land-cover reconstructions through the Holocene in southern Sweden. *Ecosystems* 24, 1450–1467. <https://doi.org/10.1007/s10021-020-00594-5/FIGURES/7>.
- Olofsson, J., Hickler, T., 2008. Effects of human land-use on the global carbon cycle during the last 6,000 years. *Veg. Hist. Archaeobotany* 605–615. <https://doi.org/10.1007/s00334-007-0126-6>.
- Opsteegh, J.D., Haarsma, R.J., Selten, F.M., Kattenberg, A., 1998. ECBILT: a dynamic alternative to mixed boundary conditions in ocean models. *Tellus Ser. A Dyn. Meteorol. Oceanogr.* 50, 348–367. <https://doi.org/10.3402/tellusa.v50i3.14524>.
- Otto, D., Rasse, D., Kaplan, J., Wamant, P., François, L., 2002. Biospheric carbon stocks reconstructed at the Last Glacial Maximum: comparison between general circulation models using prescribed and computed sea surface temperatures. *Global Planet. Change* 33, 117–138. [https://doi.org/10.1016/S0921-8181\(02\)00066-8](https://doi.org/10.1016/S0921-8181(02)00066-8).
- Pinter, N., Fiedel, S., Keeley, J.E., Pinter, N., Fiedel, S., Keeley, J.E., 2011. Fire and vegetation shifts in the Americas at the vanguard of Paleoindian migration. *QSRV* 30, 269–272. <https://doi.org/10.1016/J.QUASCIREV.2010.12.010>.
- Pirzamanbein, B., Lindström, J., 2022. Reconstruction of past human land use from pollen data and anthropogenic land cover changes. *Environmetrics* 33, e2743. <https://doi.org/10.1002/ENV.2743>.
- Pongratz, J., Reick, C., Raddatz, T., Claussen, M., 2008. A reconstruction of global agricultural areas and land cover for the last millennium. *Global Biogeochem. Cycles* 22. <https://doi.org/10.1029/2007GB003153> n/a-n/a.
- Pongratz, J., Reick, C.H., Raddatz, T., Claussen, M., 2010. Biogeophysical versus biogeochemical climate response to historical anthropogenic land cover change. *Geophys. Res. Lett.* 37. <https://doi.org/10.1029/2010GL043010>.
- Popova, S., Utescher, T., Gromyko, D.V., Mosbrugger, V., Herzog, E., François, L., 2013. Vegetation change in Siberia and the northeast of Russia during the cenozoic cooling: a study based on diversity of plant functional types. *Palaios* 28, 418–432. <https://doi.org/10.2110/palo.2012.p12-096r>.
- Poska, A., Väli, V., Vassiljev, J., Alliksaar, T., Saare, L., 2022. Timing and drivers of local to regional scale land-cover changes in the hemiboreal forest zone during the Holocene: a pollen-based study from South Estonia. *Quat. Sci. Rev.* 277, 107351. <https://doi.org/10.1016/J.QUASCIREV.2021.107351>.
- Power, M.J., Marlon, J., Ortiz, N., Bartlein, P.J., Harrison, S.P., Mayle, F.E., Ballouche, A., Bradshaw, R.H.W., Carcaillet, C., Cordova, C., Mooney, S., Moreno, P. I., Prentice, I.C., Thonicke, K., Tinner, W., Whitlock, C., Zhang, Y., Zhao, Y., Ali, A.A., Anderson, R.S., Beer, R., Behling, H., Briles, C., Brown, K.J., Brunelle, A., Bush, M., Camill, P., Chu, G.Q., Clark, J., Colombaroli, D., Connor, S., Daniau, A.L., Daniels, M., Dodson, J., Doughty, E., Edwards, M.E., Finsinger, W., Foster, D., Frechette, J., Gaillard, M.J., Gavin, D.G., Gobet, E., Haberle, S., Hallett, D.J., Higuera, P., Hope, G., Horn, S., Inoue, J., Kaltenrieder, P., Kennedy, L., Kong, Z.C., Larsen, C., Long, C.J., Lynch, J., Lynch, E.A., McGlone, M., Meeks, S., Mensing, S., Meyer, G., Minckley, T., Mohr, J., Nelson, D.M., New, J., Newnham, R., Noti, R., Oswald, W., Pierce, J., Richard, P.J.H., Rowe, C., Sanchez Goñi, M.F., Shuman, B.N., Takahara, H., Toney, J., Turney, C., Urrego-Sanchez, D.H., Umbanhowar, C., Vandergoes, M., Vanniere, B., Vescovi, E., Walsh, M., Wang, X., Williams, N., Wilmshurst, J., Zhang, J.H., 2008. Changes in fire regimes since the last glacial maximum: an assessment based on a global synthesis and analysis of charcoal data. *Clim. Dynam.* 30, 887–907. <https://doi.org/10.1007/S00382-007-0334-X/FIGURES/5>.
- Prentice, I.C., Harrison, S.P., Jolly, D., Guiot, J., 1998. The climate and biomes of Europe at 6000 yr BP: comparison of model simulations and pollen-based reconstructions. *Quat. Sci. Rev.* 17, 659–668. [https://doi.org/10.1016/S0277-3791\(98\)00016-X](https://doi.org/10.1016/S0277-3791(98)00016-X).
- Quiquet, A., Roche, D., Dumas, C., Paillard, D., Roche, D.M., 2018. Online dynamical downscaling of temperature and precipitation within the iLOVECLIM model (version 1.1) Online dynamical downscaling of temperature and precipitation within the iLOVECLIM model (version 1.1). *Geoscientific Model Development Online dynamical.* *Eur. Geosci. Union* 11, 453–466. <https://doi.org/10.5194/gmd-11-453-2018>.
- Ramankutty, N., Foley, J.A., 1999. Estimating historical changes in global land cover: croplands from 1700 to 1992. *Global Biogeochem. Cycles* 13, 997–1027. <https://doi.org/10.1029/1999GB900046>.
- Raynaud, D., Barnola, J.M., Chappellaz, J., Blunier, T., Indermühle, A., Stauffer, B., 2000. The ice record of greenhouse gases: a view in the context of future changes. *Quat. Sci. Rev.* 19, 9–17. [https://doi.org/10.1016/S0277-3791\(99\)00082-7](https://doi.org/10.1016/S0277-3791(99)00082-7).
- Ren, Z., Zhu, H., Shi, H., Liu, X., Ren, Z., Zhu, H., Shi, H., Liu, X., 2021. Shift of potential natural vegetation against global climate change under historical, current and future scenarios. *Rangel. J.* 43, 309–319. <https://doi.org/10.1071/RJ20092>.
- Roberts, C.N., Woodbridge, J., Palmisano, A., Bevan, A., Fyfe, R., Shennan, S., 2019. Mediterranean landscape change during the Holocene: synthesis, comparison and regional trends in population, land cover and climate. *Holocene* 29, 923–937. <https://doi.org/10.1177/0959683619826697/ASSET/IMAGES/LARGE/10.1177.0959683619826697-FIG7.JPG>.
- Roberts, N., Fyfe, R.M., Woodbridge, J., Gaillard, M.-J., Davis, B.A.S.S., Kaplan, J.O., Marquer, L., Mazier, F., Nielsen, A.B., Sugita, S., Trondman, A.-K.K., Leydet, M., 2018. Europe's lost forests: a pollen-based synthesis for the last 11,000 years. *Sci. Rep.* 8, 1–8. <https://doi.org/10.1038/s41598-017-18646-7>.
- Roberts, P., Buhlich, A., Caetano-Andrade, V., Cosgrove, R., Fairbairn, A., Florin, S.A., Vanwezer, N., Boivin, N., Hunter, B., Mosquito, D., Turpin, G., Ferrier, A., 2021. Reimagining the relationship between Gondwanan forests and Aboriginal land management in Australia's "Wet Tropics." *iScience* 24, 102190. <https://doi.org/10.1016/J.ISCI.2021.102190>.
- Roche, D.M., 2013. Delta O-18 water isotope in the iLOVECLIM model (version 1.0) - Part 1: implementation and verification. *Geosci. Model Dev* 6, 1481–1491. <https://doi.org/10.5194/gmd-6-1481-2013>.
- Roebroeks, W., MacDonald, K., Scherjon, F., Bakels, C., Kindler, L., Nikulina, A., Pop, E., Gaudzinski-Windheuser, S., 2021. Landscape modification by last interglacial neanderthals. *Sci. Adv.* 7, 1–14. <https://doi.org/10.1126/sciadv.abj5567>.
- Rowley-Conwy, P., Layton, R., 2011. Foraging and farming as niche construction: stable and unstable adaptations. *Philos. Trans. R. Soc. B Biol. Sci.* 366, 849–862. <https://doi.org/10.1098/RSTB.2010.0307>.
- Ruddiman, W.F., 2013. The anthropocene. *Annu. Rev. Earth Planet Sci.* 41, 45–68. <https://doi.org/10.1146/ANNUREV-EARTH-050212-123944>.
- Ruddiman, W.F., 2018. Three flaws in defining a formal 'Anthropocene'. *Prog. Phys. Geogr.* 42, 451–461. <https://doi.org/10.1177/0309133318783142/ASSET/IMAGES/LARGE/10.1177.0309133318783142-FIG3.JPG>.
- Ruddiman, W.F., Ellis, E.C., 2009. Effect of per-capita land use changes on Holocene forest clearance and CO2 emissions. *Quat. Sci. Rev.* 28, 3011–3015. <https://doi.org/10.1016/j.quascirev.2009.05.022>.
- Ruddiman, W.F., Fuller, D.Q., Kutzbach, J.E., Tzedakis, P.C., Kaplan, J.O., Ellis, E.C., Vavrus, S.J., Roberts, C.N., Fyfe, R., He, F., Lemmen, C., Woodbridge, J., 2016. Late Holocene climate: natural or anthropogenic? *Rev. Geophys.* 54, 93–118. <https://doi.org/10.1002/2015RG000503>.
- Rull, V., 2017. The "Anthropocene" uncovered. *Collect. Bot.* 36. <https://doi.org/10.3989/collectbot.2017.v36.008>.
- Sandom, C.J., Faubry, S., Sandel, B.S., Svenning, J.-C., 2014. Global Late Quaternary Megafauna Extinctions Linked to Humans, Not Climate Change, vols. 1–9. <https://doi.org/10.1098/rspb.2013.3254>.
- Scherjon, F., Bakels, C., MacDonald, K., Roebroeks, W., 2015. Burning the land: an ethnographic study of off-site fire use by current and historically documented foragers and implications for the interpretation of past fire practices in the landscape. *Curr. Anthropol.* 56, 299–326. <https://doi.org/10.1086/681561/ASSET/IMAGES/LARGE/FG7.JPG>.
- Schilt, A., Baumgartner, M., Blunier, T., Schwander, J., Spahni, R., Fischer, H., Stocker, T.F., 2010. Glacial-interglacial and millennial-scale variations in the atmospheric nitrous oxide concentration during the last 800,000 years. *Quat. Sci. Rev.* 29, 182–192. <https://doi.org/10.1016/j.quascirev.2009.03.011>.
- Seddon, A.W.R., Macias-Fauria, M., Willis, K.J., 2014. Climate and abrupt vegetation change in Northern Europe since the last deglaciation. *Holocene* 25, 25–36. <https://doi.org/10.1177/0959683614556383>.
- Serge, M.A., 2023. Spatially Extensive and Temporally Continuous Three REVEALS Pollen-Based Vegetation Reconstructions in Europe over the Holocene, Data, V1. InDoRES.
- Serge, M.A., Mazier, F., Fyfe, R., Gaillard, M.-J., Klein, T., Lagnoux, A., Galop, D., Githumbi, E., Mindrescu, M., Nielsen, A.B., Trondman, A.-K., Poska, A., Sugita, S., Woodbridge, J., 2023. Testing the effect of relative pollen productivity on the REVEALS model. A Validated Reconstruction of Europe-Wide Holocene Vegetation. *L. 2023* 12, 986. <https://doi.org/10.3390/LAND12050986>, 12, Page 986.
- Shennan, S., Downey, S.S., Timpson, A., Edinborough, K., Colledge, S., Kerig, T., Manning, K., Thomas, M.G., 2013. Regional population collapse followed initial agriculture booms in mid-Holocene Europe. *Nat. Commun.* 2013 41, 1–8. <https://doi.org/10.1038/ncomms3486>.
- Smith, B.D., Zeder, M.A., 2013. The onset of the Anthropocene. *Anthropocene* 4, 8–13. <https://doi.org/10.1016/J.ANCENE.2013.05.001>.
- Smith, M.C., Singarayer, J.S., Valdes, P.J., Kaplan, J.O., Branch, N.P., 2016. The biogeophysical climatic impacts of anthropogenic land use change during the Holocene. *Clim. Past* 12, 923–941. <https://doi.org/10.5194/cp-12-923-2016>.
- Somodi, I., Molnár, Z., Ewald, J., 2012. Towards a more transparent use of the potential natural vegetation concept – an answer to Chiarucci et al. *J. Veg. Sci.* 23, 590–595. <https://doi.org/10.1111/J.1654-1103.2011.01378.X>.
- Steffen, W., Grinevald, J., Crutzen, P., McNeill, J., 2011. The Anthropocene: conceptual and historical perspectives. *Philos. Trans. R. Soc. A Math. Phys. Eng. Sci.* 369, 842–867. <https://doi.org/10.1098/RSTA.2010.0327>.
- Stephens, L., Fuller, D., Boivin, N., Rick, T., Gauthier, N., Kay, A., Marwick, B., Armstrong, C.G.D., Barton, C.M., Denham, T., Douglass, K., Driver, J., Janz, L.,

- Roberts, P., Rogers, J.D., Thakar, H., Johnson, A.L., Vattuone, M.M.S., Aldenderfer, M., Archila, S., Artioli, G., Bale, M.T., Beach, T., Borrell, F., Braje, T., Buckland, P.I., Cano, N.G.J., Capriles, J.M., Castillo, A.D., Çilingiroğlu, Ç., Cleary, M. N., Conolly, J., Coutros, P.R., Covey, R.A., Cremaschi, M., Crowther, A., Der, L., di Lernia, S., Doershuk, J.F., Doolittle, W.E., Edwards, K.J., Erlandson, J.M., Evans, D., Fairbairn, A., Faulkner, P., Feinman, G., Fernandes, R., Fitzpatrick, S.M., Fyfe, R., Garcea, E., Goldstein, S., Goodman, R.C., Guedes, J.D., Herrmann, J., Hiscock, P., Hommel, P., Horsburgh, K.A., Hritz, C., Ives, J.W., Junno, A., Kahn, J.G., Kaufman, B., Kearns, C., Kidder, T.R., Lanoë, F., Lawrence, D., Lee, G.A., Levin, M.J., Lindskoug, H.B., López-Sáez, J.A., Macrae, S., Marchant, R., Marston, J.M., McClure, S., McCoy, M.D., Miller, A.V., Morrison, M., Matuzeviciute, G.M., Müller, J., Nayak, A., Noerwidi, S., Peres, T.M., Peterson, C.E., Proctor, L., Randall, A.R., Renette, S., Schug, G.R., Ryzewski, K., Saini, R., Scheinsohn, V., Schmidt, P., Sebillaud, P., Simpson, I.A., Sołtyśiak, A., Speakman, R.J., Spengler, R. N., Steffen, M.L., Storozum, M.J., Strickland, K.M., et al., 2019. Archaeological assessment reveals Earth's early transformation through land use. *Science* 84 365, 897–902. <https://doi.org/10.1126/science.aax1192>.
- Stewart, M., Carleton, W.C., Groucutt, H.S., 2021. Climate change, not human population growth, correlates with Late Quaternary megafauna declines in North America. *Nat. Commun.* 12, 1–15. <https://doi.org/10.1038/s41467-021-21201-8>.
- Stocker, B.D., Strassmann, K., Joos, F., 2011. Sensitivity of Holocene atmospheric CO<sub>2</sub> and the modern carbon budget to early human land use: analyses with a process-based model. *Biogeosciences* 8, 69–88. <https://doi.org/10.5194/bg-8-69-2011>.
- Strandberg, G., Lindström, J., Poska, A., Zhang, Q., Fyfe, R., Githumbi, E., Kjellström, E., Mazier, F., Nielsen, A.B., Sugita, S., Trondman, A.K., Woodbridge, J., Gaillard, M.J., 2022. Mid-Holocene European climate revisited: new high-resolution regional climate model simulations using pollen-based land-cover. *Quat. Sci. Rev.* 281, 107431 <https://doi.org/10.1016/j.quascirev.2022.107431>.
- Strona, G., Mauri, A., Veech, J.A., Seufert, G., Ayaz, J.S.M., Fattorini, S., 2016. Far from naturalness: how much does spatial ecological structure of European tree assemblages depart from potential natural vegetation? *PLoS One* 11, e0165178. <https://doi.org/10.1371/JOURNAL.PONE.0165178>.
- Stuart, A., Ord, J.K., 1994. Kendall's advanced theory of statistics. *Distribution theory, Sci. Res. Publ.* 1.
- Sugita, S., 2007, 10.1177/0959683607075837, 17229–241. <https://doi.org/10.1177/0959683607075837>.
- Sun, Y., Xu, Q., Gaillard, M.J., Zhang, S., Li, D., Li, M., Li, Y., Li, X., Xiao, J., 2022. Pollen-based reconstruction of total land-cover change over the Holocene in the temperate steppe region of China: an attempt to quantify the cover of vegetation and bare ground in the past using a novel approach. *Catena* 214, 106307. <https://doi.org/10.1016/j.catena.2022.106307>.
- Swindles, G.T., Roland, T.P., Ruffell, A., 2023. The 'Anthropocene' is most useful as an informal concept. *J. Quat. Sci.* 38, 453–454. <https://doi.org/10.1002/jqs.3492>.
- Tarasov, L., Peltier, W.R., 2002. Greenland glacial history and local geodynamic consequences. *Geophys. J. Intell.* 150, 198–229. <https://doi.org/10.1046/j.1365-246x.2002.01702.x/2/150-1-198-FIG015.JPEG>.
- Tarasov, L., Dyke, A.S., Neal, R.M., Peltier, W.R., 2012. A data-calibrated distribution of deglacial chronologies for the North American ice complex from glaciological modeling. *Earth Planet. Sci. Lett.* 315, 30–40. <https://doi.org/10.1016/j.epsl.2011.09.010>. –316.
- Trondman, A.-K.K., Gaillard, M.-J., Mazier, F., Sugita, S., Fyfe, R., Nielsen, A.B., Twiddle, C., Barratt, P., Birks, H.J.B., Björkman, A.E., Björkman, L., Broström, A., Caseldine, C., David, R., Dodson, J., Dörfler, W., Fischer, E., van Geel, B., Giesecke, T., Hultberg, T., Kalnina, L., Kangur, M., van der Knaap, P., Koff, T., Kuneš, P., Lagerås, P., Latalowa, M., Lechterbeck, J., Leroyer, C., Leydet, M., Lindbladh, M., Marquer, L., Mitchell, F.J.G.G., Odgaard, B.V., Peglar, S.M., Persson, T., Poska, A., Rösch, M., Seppä, H., Veski, S., Wick, L., 2015. Pollen-based quantitative reconstructions of Holocene regional vegetation cover (plant-functional types and land-cover types) in Europe suitable for climate modelling. *Global Change Biol.* 21, 676–697. <https://doi.org/10.1111/gcb.12737>.
- Vannièr, B., Blarquez, O., Rius, D., Doyen, E., Brücher, T., Colombaroli, D., Connor, S., Feurdean, A., Hickler, T., Kaltenrieder, P., Lemmen, C., Leys, B., Massa, C., Olofsson, J., 2016. 7000-year human legacy of elevation-dependent European fire regimes. *Quat. Sci. Rev.* 132, 206–212.
- Vavrus, S.J., Kucharik, C.J., He, F., Kutzbach, J.E., Ruddiman, W.F., 2022. Did agriculture beget agriculture during the past several millennia? *Holocene* 32, 680–689. [https://doi.org/10.1177/09596836221088231/ASSET/IMAGES/LARGE/10.1177\\_09596836221088231-FIG2.JPEG](https://doi.org/10.1177/09596836221088231/ASSET/IMAGES/LARGE/10.1177_09596836221088231-FIG2.JPEG).
- Vrac, M., 2018. Multivariate bias adjustment of high-dimensional climate simulations: the Rank Resampling for Distributions and Dependencies (R2D2) bias correction. *Hydrol. Earth Syst. Sci.* 22, 3175–3196. <https://doi.org/10.5194/hess-22-3175-2018>.
- Vrac, M., Drobinski, P., Merlo, A., Herrmann, M., Lavaysse, C., Li, L., Somot, S., 2012. Dynamical and statistical downscaling of the French Mediterranean climate: uncertainty assessment. *Nat. Hazards Earth Syst. Sci.* 12, 2769–2784. <https://doi.org/10.5194/nhess-12-2769-2012>.
- Warnant, P., François, L.M., Strivay, D., Gérard, J.-C., 1994. CARAIB: a global model of terrestrial biological productivity. *Global Biogeochem. Cycles* 8, 255–270. <https://doi.org/10.1029/94GB00850>.
- Waters, C.N., Zalasiewicz, J., Summerhayes, C., Barnosky, A.D., Poirier, C., Galuszka, A., Cearreta, A., Edgeworth, M., Ellis, E.C., Ellis, M., Jeandel, C., Leinfelder, R., McNeill, J.R., Richter, D.D.B., Steffen, W., Syvitski, J., Vidas, D., Waple, M., Williams, M., Zhisheng, A., Grinevald, J., Odada, E., Oreskes, N., Wolfe, A.P., 2016. The Anthropocene is functionally and stratigraphically distinct from the Holocene. *Science* (80-), 351. <https://doi.org/10.1126/science.aad2622> aad2622–aad2622.
- Williams, M., Zalasiewicz, J., Haff, P.K., Schwägerl, C., Barnosky, A.D., Ellis, E.C., 2015. The anthropocene biosphere. <https://doi.org/10.1177/2053019615591020>, 18 December.
- Woodbridge, J., Fyfe, R., Roberts, C., Trondman, A., Mazier, F., Davis, B., 2018. European forest cover since the start of Neolithic agriculture: a critical comparison of pollen-based reconstructions. *Past Glob. Chang. Mag.* 26, 10–11. <https://doi.org/10.22498/pages.26.1.10>.
- Zalasiewicz, J., Waters, C.N., Ellis, E.C., Head, M.J., Vidas, D., Steffen, W., Thomas, J.A., Horn, E., Summerhayes, C.P., Leinfelder, R., McNeill, J.R., Galuszka, A., Williams, M., Barnosky, A.D., Richter, D. de B., Gibbard, P.L., Syvitski, J., Jeandel, C., Cearreta, A., Cundy, A.B., Fairchild, L.J., Rose, N.L., Sul, J. A. I. do, Shoyk, W., Turner, S., Waple, M., Zinke, J., 2021. The anthropocene: comparing its meaning in geology (chronostratigraphy) with conceptual approaches arising in other disciplines. *Earth's Future* 9, e2020EF001896. <https://doi.org/10.1029/2020EF001896>.
- Zapolska, A., Vrac, M., Quiquet, A., Extier, T., Arthur, F., Renssen, H., Roche, D.M., 2023. Improving biome and climate modelling for a set of past climate conditions: evaluating bias correction using the CDF-t approach. *Environ. Res. Clim.* 2, 25004 <https://doi.org/10.1088/2752-5295/ACCBE2>.
- Zhang, Y., Renssen, H., Seppä, H., Valdes, P.J., 2017. Holocene temperature evolution in the Northern Hemisphere high latitudes – model-data comparisons. *Quat. Sci. Rev.* 173, 101–113. <https://doi.org/10.1016/j.quascirev.2017.07.018>.